NAVAL POSTGRADUATE SCHOOL
Monterey, California

THESIS

EXPERIMENTAL INVESTIGATION OF TURBULENT HEAT TRANSFER IN STRAIGHT AND CURVED RECTANGULAR DUCTS

by

Steven Floyd Daughety

September 1983

Thesis Advisor M. D. Kelleher

Approved for public release; distribution unlimited.

REPORT DOCUMENTATION PAGE

READ INSTRUCTIONS BEFORE COMPLETING FORM

1. REPORT NUMBER

2. GOVT ACCESSION NO.

3. RECIPIENT'S CATALOG NUMBER

4. TITLE (and Subtitle)
Experimental Investigation of Turbulent Heat Transfer in Straight and Curved Rectangular Ducts

5. TYPE OF REPORT & PERIOD COVERED
Master's Thesis
September 1983

6. PERFORMING ORG. REPORT NUMBER

7. AUTHOR(s)
Steven Floyd Daughety

8. CONTRACT OR GRANT NUMBER(s)

9. PERFORMING ORGANIZATION NAME AND ADDRESS
Naval Postgraduate School
Monterey, California 93943

10. PROGRAM ELEMENT, PROJECT, TASK AREA & WORK UNIT NUMBERS

11. CONTROLLING OFFICE NAME AND ADDRESS
Naval Postgraduate School
Monterey, California 93943

12. REPORT DATE
September 1983

13. NUMBER OF PAGES
73

14. MONITORING AGENCY NAME & ADDRESS(if different from Controlling Office)

15. SECURITY CLASS. (of this report)
Unclassified

15a. DECLASSIFICATION/DOWNGRADING SCHEDULE

16. DISTRIBUTION STATEMENT (of this Report)
Approved for public release; distribution unlimited.

17. DISTRIBUTION STATEMENT (of the abstract entered in Block 20, if different from Report)

18. SUPPLEMENTARY NOTES

19. KEY WORDS (Continue on reverse side if necessary and identify by block number)
Taylor-Gortler Vortices, heat transfer, secondary flow, rectangular curved channel, rectangular straight channel, Temsheet, Joulean heating, turbulent flow.

20. ABSTRACT (Continue on reverse side if necessary and identify by block number)
An experimental investigation was conducted to examine the convective heat transfer in straight and curved ducts of rectangular cross-section. The experimental configuration was modeled as infinite parallel plates with one wall at a constant temperature and the opposite wall adiabatic.

Item #20 continued:

The experiments were conducted at steady state for turbulent flow. Average Nusselt numbers were used to compare the heat transfer characteristics of the straight and curved sections. The development of Taylor-Gortler vortices in the curved section was shown to enhance the heat transfer rate in the curved section as compared to that of the straight section by approximately 15 to 20 percent. Improved heat exchanger designs and improved cooling of turbine blades are two disciplines that could benefit from a better understanding of the effects of curvature on the rate of heat transfer.

Approved for public release; distribution unlimited.

Experimental Investigation of Turbulent Heat Transfer in Straight and Curved Rectangular Ducts

by

Steven Floyd Daughety
Lieutenant, United States Navy
B.S., United States Naval Academy, 1976

Submitted in partial fulfillment of the
requirements for the degree of

MASTER OF SCIENCE IN MECHANICAL ENGINEERING

from the

NAVAL POSTGRADUATE SCHOOL
September 1983

ABSTRACT

An experimental investigation was conducted to examine the convective heat transfer in straight and curved ducts of rectangular cross-section. The experimental configuration was modeled as infinite parallel plates with one wall at a constant temperature and the opposite wall adiabatic.

The experiments were conducted at steady state for turbulent flow. Average Nusselt numbers were used to compare the heat transfer characteristics of the straight and curved sections. The development of Taylor-Gortler vortices in the curved section was shown to enhance the heat transfer rate in the curved section as compared to that of the straight section by approximately 15 to 20 percent. Improved heat exchanger designs and improved cooling of turbine blades are two disciplines that could benefit from a better understanding of the effects of curvature on the rate of heat transfer.

TABLE OF CONTENTS

LIST OF TABLES

LIST OF FIGURES

TABLE OF SYMBOLS

Symbol	Meaning	Units
A	cross-sectional area of the orifice	m^2
A_c	cross-sectional area of the channel	m^2
A_{pipe}	cross-sectional area of the pipe	m^2
A_{PL}	area of the wall heater (Temsheet)	m^2
C_{pair}	specific heat of air at constant pressure	J/KgK
Dc	channel height	m
De	Dean number	
D_{hd}	hydraulic diameter	m
D_{orif}	diameter of the orifice	m
D_{pipe}	diameter of the pipe	m
F_{wo-wi}	radiation shape factor	
g_c		$\frac{Kg\ m}{N\ sec^2}$
$\bar{h}$	average heat transfer coefficient	W/m^2C
K	flow coefficient	
K_{air}	thermal conductivity of air	W/mC
K_{ins}	thermal conductivity of insulation	W/mC
$\dot{m}$	mass flow rate of air	Kg/sec
Nu	local Nusselt number	
$\overline{Nu}$	average Nusselt number	
Pr	Pradtl number	
P_{atm}	atmospheric pressure	N/m^2
P_1	pressure upstream of orifice	N/m^2

Symbol	Meaning	Units
P_{wet}	wetted perimeter of channel	m
Q_{air}	heat convected to the air	W
Q_{li}	heat lost through inner wall (Plexiglas)	W
Q_{lo}	heat lost through outer wall (Temsheet)	W
Q_p	power supplied	W
Q_r	heat transferred by radiation	W
R	gas constant for air	Nm/Kg K
Re_d	Reynolds number based on channel height	
Re_{hd}	Reynolds number based on hydraulic diameter	
Re_{pipe}	Reynolds number based on pipe diameter	
Ri	radius of curvature of inner convex wall	m
R_{PR}	electrical resistance of precision resistor	Ω
R_R	total radiation resistance	m^{-2}
Ta	Taylor number	
T_{blk}	bulk temperature of flow	C
T_{in}	average flow inlet temperature	C
T_{insl}	temperature between first and second layers of insulation	C
T_{ins2}	temperature between second and third layers of insulation	C
T_{orif}	temperature of air flowing downstream of orifice	C
T_{out}	average flow outlet temperature	C
T_{wi}	average temperature of inner wall	C
T_{wo}	average temperature of outer wall	C

Symbol	Meaning	Units
V_{PR}	voltage across precision resistor	V
V_H	voltage across the wall heater (Temsheet)	V
Y	expansion factor	
β	ratio of orifice diameter to pipe diameter	
ε_{wi}	emissivity of inner wall (Plexiglas)	
ε_{wo}	emissivity of outer wall (Temsheet)	
γ	ratio of specific heats of air	
μ_{air}	dynamic viscosity of air	Kg/m sec
ρ_{air}	density of air	Kg/m^3
ρ	Stefan-Boltzmann constant	W/m^2K^4
ΔP	pressure drop across the orifice	N/m^2
ΔT	mean temperature difference	C
ΔT_{ins}	temperature difference in insulation	C
ΔX_{ins}	thickness of insulation layers	m

ACKNOWLEDGEMENT

The author wishes to express his sincere appreciation to Professor Matthew D. Kelleher for his guidance and assistance throughout the execution of this project, without which this thesis would have been an insurmountable task.

The shop personnel also deserve a special thanks for their assistance in making the necessary modifications required to accomplish this experiment.

Finally, the author wishes to thank his wife Beth for her understanding and encouragement throughout the entire tour of duty in Monterey.

I. INTRODUCTION

A. TAYLOR-GORTLER VORTICES

Since the early part of the twentieth century, considerable research has shown that fully developed laminar flow along a concave wall does not remain two-dimensional [Refs. 1, 2, 3]. The flow instead forms a system of spiral vortices, of counter rotating pairs, whose axes are in the principle flow direction. This phenomenon is the result of the variations in the centrifugal forces acting on the fluid particles, and is known as Taylor-Gortler vortices. Figures 1 and 2 illustrate the type of fluid motion just described.

In a channel that is curved in the streamwise direction, those fluid particles located in the center of the flow cross-section are subjected to higher centrifugal forces than those fluid particles traveling along the channel's boundary wall. As a result, the fluid in the center of the channel moves outwardly towards the concave boundary. As the process continues, the fluid particles near the boundary wall, move in a spanwise direction, and finally radially inward replacing the outwardly moving particles. These particles then come under the same centrifugal forces and the process repeats itself. The resulting cyclic motion, causes the formation, and propagation, of the counter-rotating Taylor-Gortler vortices which are considered primarily a laminar flow phenomenon.

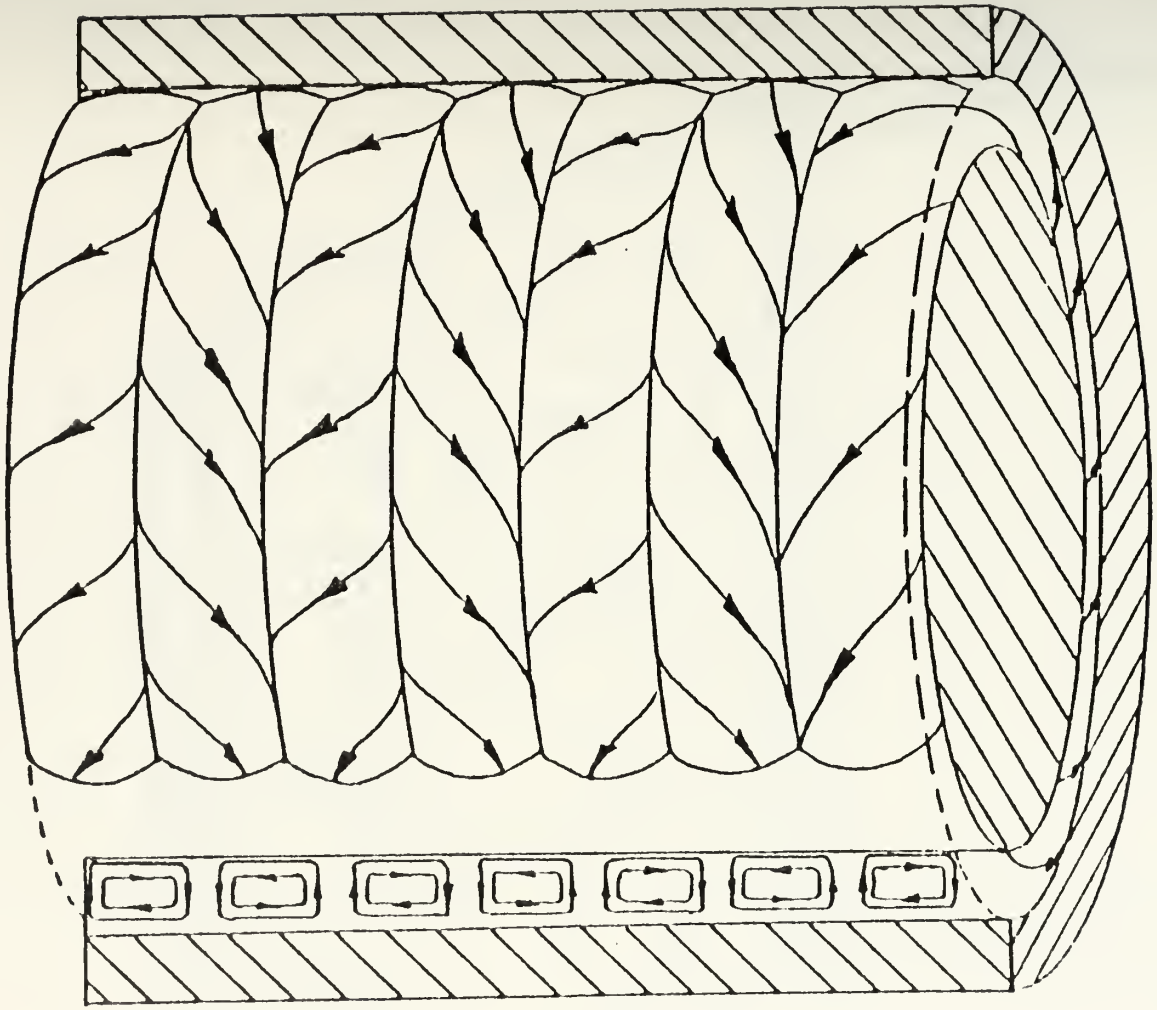

Figure 1. Schematic of Taylor vortices between cylinders.

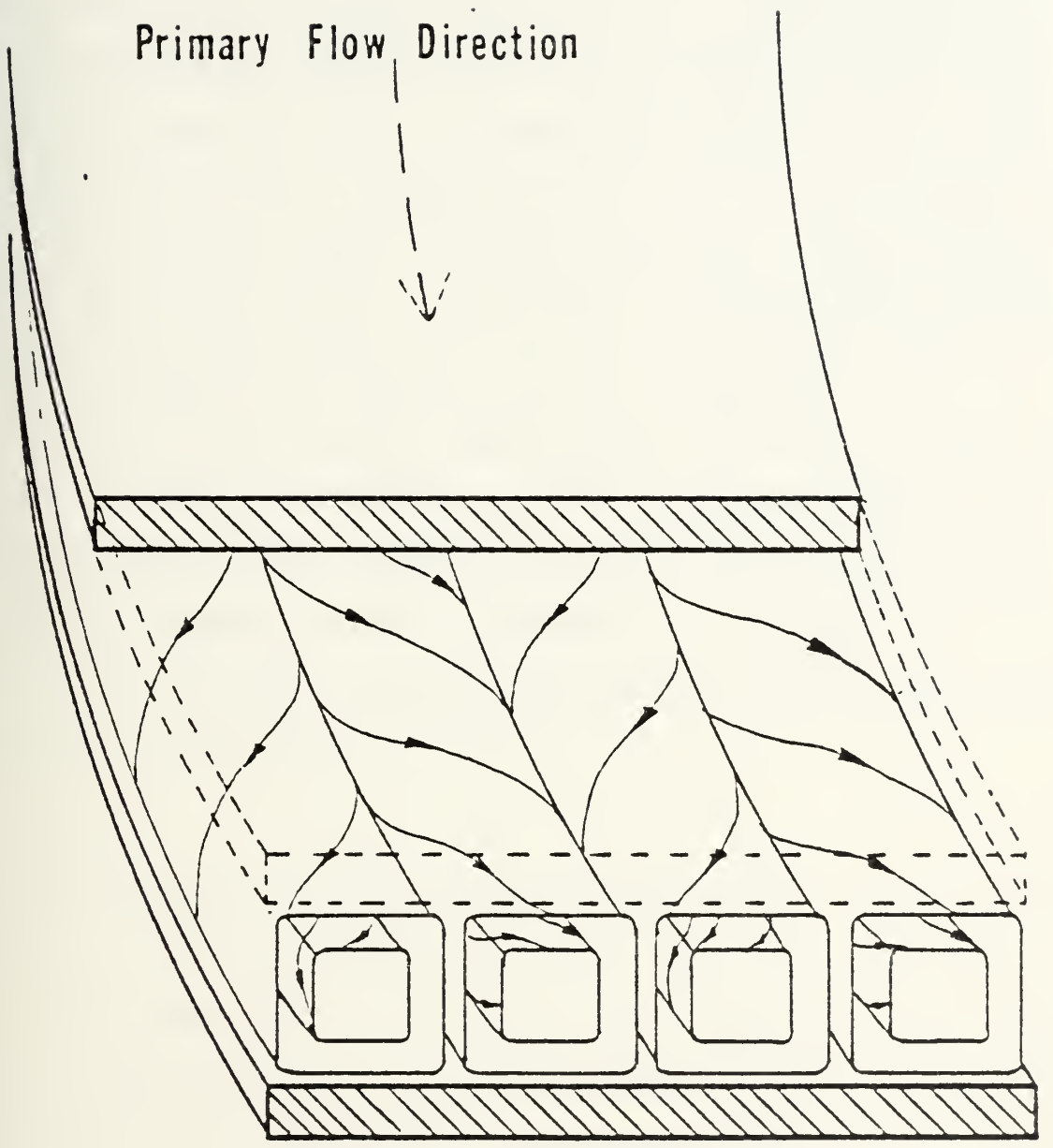

Figure 2. Schematic of Taylor-Gortler vortices in a curved channel.

It has been observed [Ref. 4] that the heat transfer rate from flow along a concave curved wall is greater than that for flow along a straight wall. It is thought that the additional mixing provided by the secondary motion of the Taylor-Gortler vortices may account for this. It is also thought that the cross-hatching that has been observed in reentry vehicles can be explained in part by the presence of streamwise vortices similar to the Taylor-Gortler vortice phenomenon.

There are many possible applications that could result from a more thorough understanding of Taylor-Gortler vortices and their effect on heat transfer and fluid flow characteristics. By taking advantage of the increased heat transfer rate, improved heat exchanger designs and improved turbine blade cooling could result [Refs. 5, 6, 7].

B. HISTORY

The instability of an inviscid fluid flowing past a curved boundary, was first considered by Lord Rayleigh in 1916 [Ref. 8]. By assuming that the fluid was non-viscous, he determined that for the motion of an inviscid fluid to remain stable, its circulation must increase with increasing radius. G. I. Taylor, in 1923, [Refs. 1, 9], continued this study with an extensive analytical and experimental study of viscous fluids. His investigations focused on the flow between two cylinders. For the case where the inner cylinder was rotated while the outer cylinder was held stationary, Taylor ascertained that such

flows become unstable when the value of a dimensionless parameter exceeded a critical value of 41.3. The parameter, known as the Taylor number is defined as:

$$Ta = Re \sqrt{\frac{d}{Ri}}$$

where 'd' is the width of the gap, assumed small when compared to 'Ri', the radius of the inner cylinder, and 'Re' is the Reynolds number. The Reynolds number is based on the peripheral velocity of the inner cylinder. Taylor determined that for those cases in which the value of the Taylor number exceeded 41.3, a secondary motion developed and the Taylor vortices formed.

Instability of a similar nature is also observed when a viscous fluid flows in a curved channel due to a pressure gradient acting along the channel wall. This problem was first considered analytically by W. R. Dean [Ref. 10] in 1928, for a channel formed by two concentric cylinders, where the radius of the innder cylinder was large in comparison to the spacing between the inner and outer cylinder walls. Dean concluded that there would be an initiation of the flow instability, and the propagation of vortices, when a similar dimensionless parameter, the Dean number, exceeded a value of 36. The Dean number is defined as:

$$De = Re \sqrt{\frac{d}{Ri}}$$

where 'd' represents the channel half-width, 'Ri' is the inner cylinder radius, and 'Re' is the Reynolds number based on the mean velocity of the undisturbed flow. The analytical work of Dean was later verified by W. H. Reid [Ref. 11], using an approximate solution.

In 1940, H. Gortler studied the stability of laminar boundary layer profiles on curved walls under the influence of small disturbances. He found that these disturbances were similar to the vortices studied by G. I. Taylor. By approximate numerical calculations, Gortler concluded that the disturbances or vortices were produced only on the concave boundary walls. He also concluded that the overall flow profile appeared to remain laminar in nature [Ref. 2]. These results were verified, with an exact solution, by G. Hammerlin, and reported by H. Schlichting [Ref. 12] in 1955. A. M. O. Smith completed an even more extensive numerical analysis that further substantiated these findings [Ref. 3]. Recently with the use of hot wire anemometry, laser doppler systems, and flow visualization techniques, [Ref. 13, 14], the result of these numerical solutions have been demonstrated experimentally. In 1976, Y. Aihara [Ref. 15] conducted a non-linear analysis of Gortler vortices.

As interest began to develop concerning the effects of the secondary flows associated with the Taylor-Gortler vortices, many studies were published concerning the influences of these vortices on the transfer of heat in the laminar and turbulent flow regimes. In 1955, F. Kreith [Ref. 16], studied the

influence of heat transfer with respect to the curvature of the boundary wall for fully turbulent flows. He concluded that the heat transfer from the heated concave boundary wall was considerably higher than that transferred from the convex boundary wall of the same curvature and under similar turbulent conditions.

In 1965, L. Persen [Ref. 17], considered the special cases of very high and very low Prandtl number fluids. He related the increase in heat transfer from a curved wall to the presence of the Taylor-Gortler vortices.

There has been only a limited amount of published literature dealing with the flow and heat transfer in curved channels of rectangular cross-section and large aspect ratios. Much of what has been published involves the development of numerical approximations and solutions for heat and mass transfer in curved ducts of various geometries. K. Cheng and M. Akiyama [Ref. 18] developed a numerical solution for forced convection heat transfer with laminar flows in curved channels of rectangular cross-section. However, they were concerned with cross-sections with small aspect ratios.

In 1976, A. A. Shibani and M. N. Ozisik [Ref. 19] solved the heat transfer problem between parallel plates with turbulent flow, for the case of uniform wall temperature. They used matched asymptotic expansion techniques for a wide range of Prandtl numbers.

Other experimental and analytical studies that are worth citing with regard to this present study follow. Y. Mori [Ref. 20], obtained results for hydrodynamically fully developed flows with constant wall heat flux, in curved channels of square cross-section. W. M. Kays and E. Y. Leung [Ref. 21] reported solutions for turbulent flow heat transfer in a concentric circular tube annulus with a fully developed velocity profile and constant heat rate per unit length, for a fluid of Prandtl number 0.7. Results for large aspect ratio channels with rectangular cross-sections for laminar flows were reported by M. Durao [Ref. 22] and J. Ballard [Ref. 23], while R. Holihan, Jr. reported results for laminar and transition flows [Ref. 24]. P. F. Brinich and R. W. Graham [Ref. 25], reported results for turbulent flows in a rectangular curved channel with an aspect ratio of 6, for the inner wall heated, the outer wall heated, and both walls heated.

II. INTENT OF THE STUDY

The purpose of this investigation was to examine the effect of streamwise curvature on the heat transfer rate in a curved rectangular duct of large aspect ratio. The flow velocities examined were in the turbulent regime. The results of this study were compared to the heat transfer rates for the same range of velocities, in a straight duct of identical aspect ratio.

Taylor-Gortler vortices are considered to be a laminar flow phenomenon. Enhanced heat transfer in curved channels for transition and turbulent flows has been observed. Even though it has not been proven that the vortices continue to propagate at the higher flow velocities, this enhancement in the transfer of heat has been attributed to the secondary flow velocity components of the Taylor-Gortler vortices. It is believed that these secondary components transport the heated fluid from the outer concave wall, inward toward the opposite wall of the channel, displacing the cooler fluid particles and causing them to move toward the heated concave wall. It was expected that similar results would be observed in this study.

This investigation was conducted using a single channel with a rectangular cross-section and constant aspect ratio. The channel incorporated both a straight test section and a

curved test section. The results obtained in each test section at approximately the same flow rates were compared in an effort to determine the effects of the Taylor-Gortler vortices on the transfer of heat. Also, the results of both the straight and curved sections were compared to the results of Ballard [Ref. 23] and Holihan [Ref. 24].

The straight section results of this study were compared to the results of Shibani and Ozisik [Ref. 19] for turbulent flow between parallel plates. In addition, the results of Kays and Leung [Ref. 21] and the Dittus-Boelter equation [Ref. 26] were compared for Reynolds numbers in the range of this study. Kays and Leung's data was for turbulent flow in annular passages while the Dittus-Boelter equation was for turbulent flows in circular tubes.

The curved section results of this study were compared with the results of Brinich and Graham [Ref. 25] for turbulent flow in a rectangular curved channel.

III. EXPERIMENTAL WORK

A. DESCRIPTION OF THE APPARATUS

To meet the objectives of this investigation, a channel of rectangular cross-section was used. Details of its construction are described in references 22 and 23. Plexiglas, 0.635 centimeters thick, formed the inner and outer walls of the channel. These walls were separated by 0.635 centimeter spacers that also served as the sides of the channel.

The channel, shown in Figure 3, had a straight section, 122.0 centimeters in length, followed by a curved section of 180 degrees of arc, followed by another straight section, 91.4 centimeters in length. The inner curved wall of the channel had a radius of curvature of 30.5 centimeters. The rectangular channel was .635 centimeters high and 25.4 centimeters wide resulting in an aspect ration of 40. The hydraulic diameter was 1.229 centimeters. The cross-sectional area of the channel was 16.13 square centimeters. The wetted perimeter was 52.07 centimeters. Figure 4 shows a cross-sectional view of both the straight and curved sections of the channel.

An entrance bell constructed of plexiglas was connected to the straight section of the channel. It was designed and manufactured according to ASME nozzle standards, with an elliptical curved base on a major axis equal to ten inches and a minor axis of one inch. Cheese-cloth was attached to

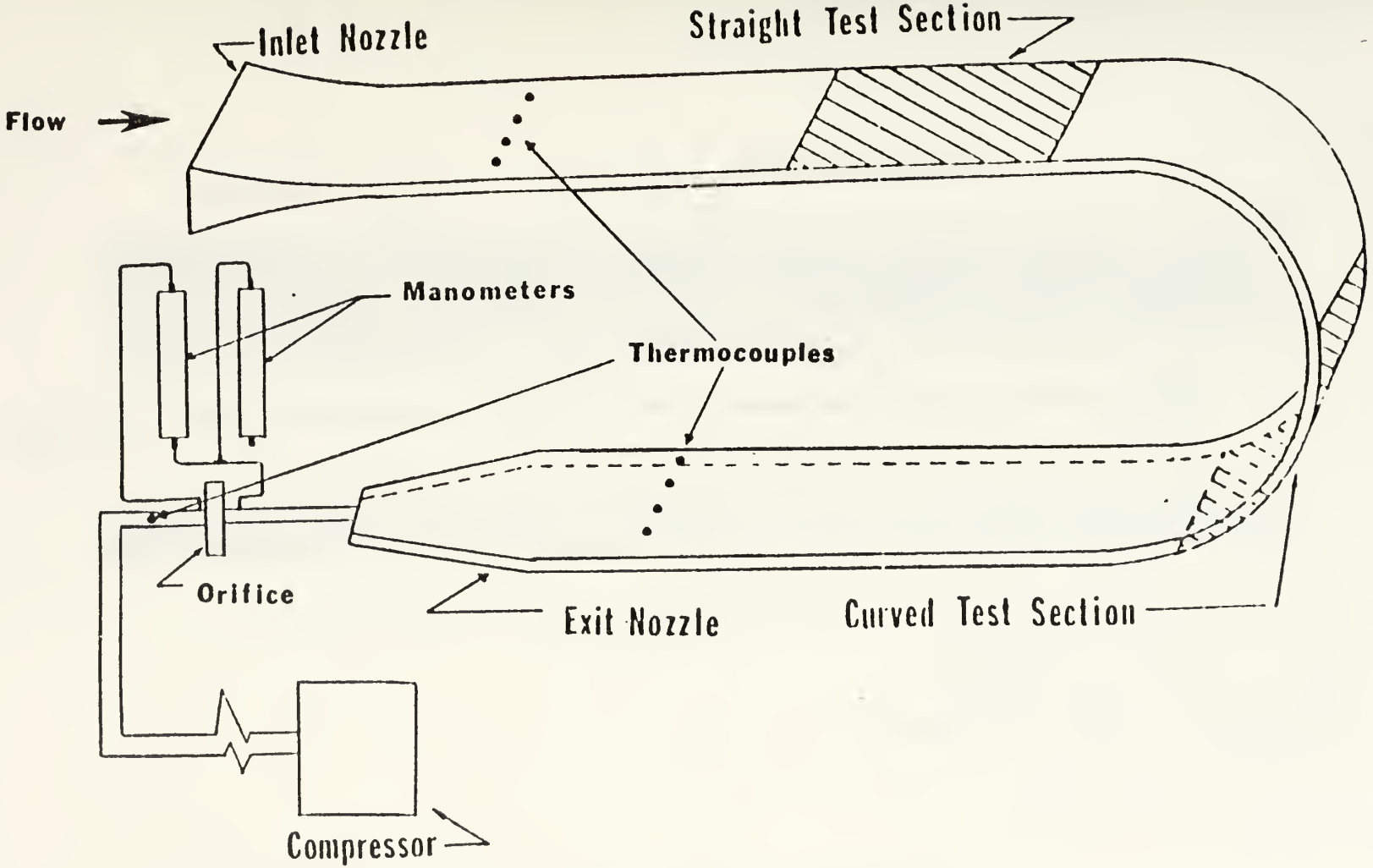

Figure 3. Illustration of equipment and apparatus.

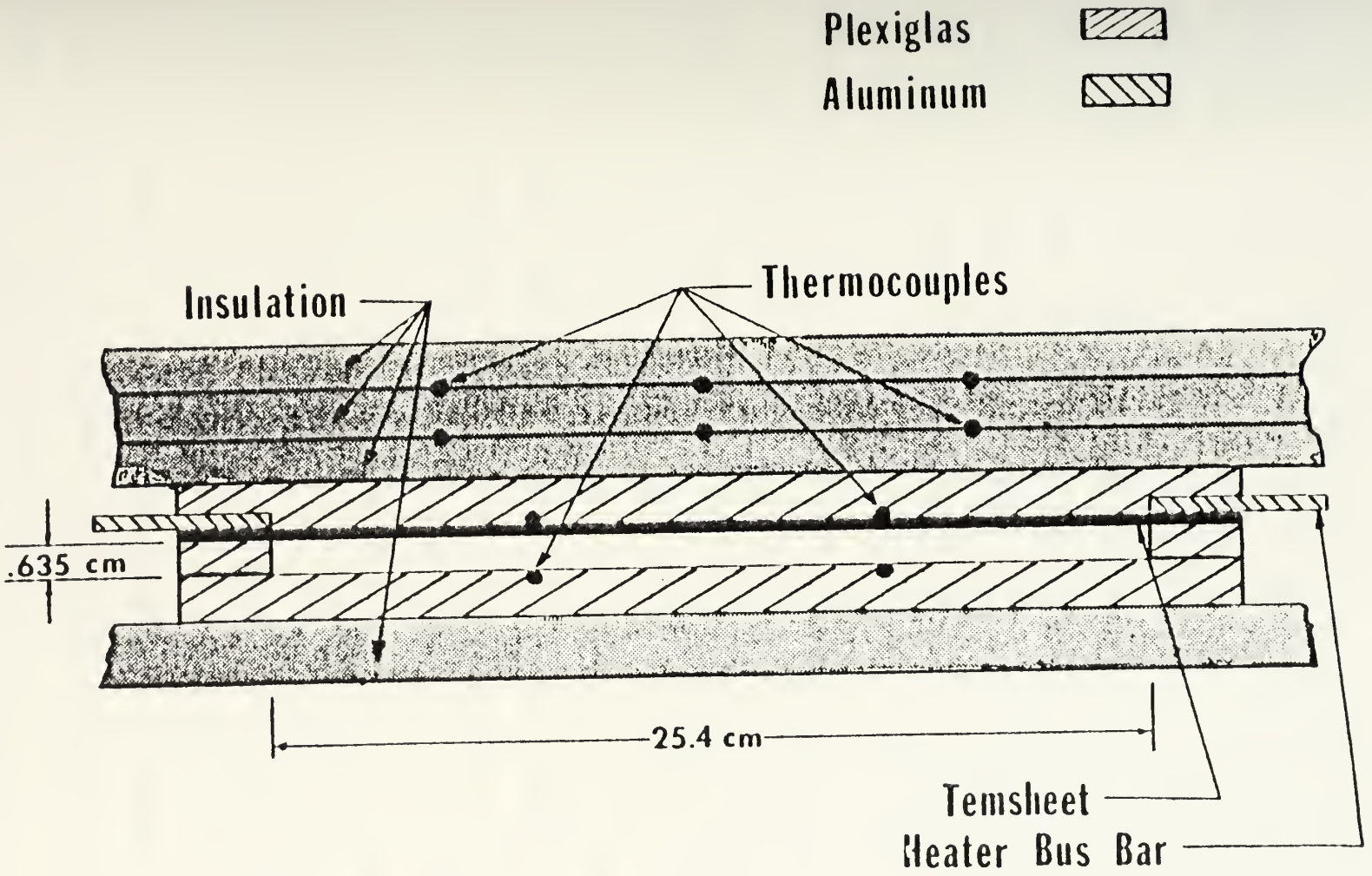

Figure 4. Cross-sectional view of channel.

the entrance nozzle to prevent foreign matter from entering the flow channel. An aluminum exhaust nozzle was attached to the exit of the channel and directed the flow from the channel into two inch diameter pvc piping. The two inch pvc piping contained a concentric orifice with a diameter of 1.065 inches and was constructed according to the ASME Power Test Code. Pressure taps on either side of the orifice, at 1 and 1/2 pipe diameters from the orifice, and connected to manometers were used to calculate the mass flow rate, of the working fluid, which was air at room temperature.

The flow of air was drawn through the channel by an electrically driven Spencer Turbo Compressor, 30 horsepower at 3500 rpm, rated at 550 cubic feet per minute at 70 degrees fahrenheit and one atmosphere. The channel contained two test sections from which experimental heat transfer data could be obtained. The straight test section was located at a distance downstream of the entrance bell that would ensure hydrodynamically fully developed flow. The straight test section was 29.2 centimeters in length with a heated test section area of 741.7 square centimeters. The curved test section was located in the lower half of the curved portion of the channel. It was 28.3 centimeters in length, subtending an arc of 53.1 degrees, and having a heated test section area of 718.4 square centimeters.

In each of the heated test sections, Temsheet, a carbon impregnated porous paper with a uniform electrical resistivity,

was glued to the outer wall of each section. Joulean heating was used to heat the flow of air through the channel. Since the electrical resistance of the Temsheet is not constant, but varies slowly with temperature, a precision resistor with an electrical resistance of 2.0262 ohms was connected in series with the Temsheet to allow the calculation of the instantaneous power being supplied. Detailed schematics of each test section are shown in Figures 5 and 6.

The variables that were measured and used in this investigation were:

(1) the temperature of the air entering the channel (T_{in})

(2) the temperature of the air leaving the channel (T_{out})

(3) the temperature of the heated outer wall for each test section (T_{wo})

(4) the temperature of the unheated inner wall for each test section (T_{wi})

(5) the temperature between the three layers of insulation at each test section (T_{ins})

(6) the voltage across the precision resistor (V_r)

(7) the voltage across the Temsheet or heater (V_h)

(8) the temperature of the air at the orifice (T_{orif})

(9) the pressure upstream of the orifice (P_{up})

(10) the difference in the upstram and the downstream pressure across the orifice (ΔP)

(11) the atmospheric pressure (P_{atm})

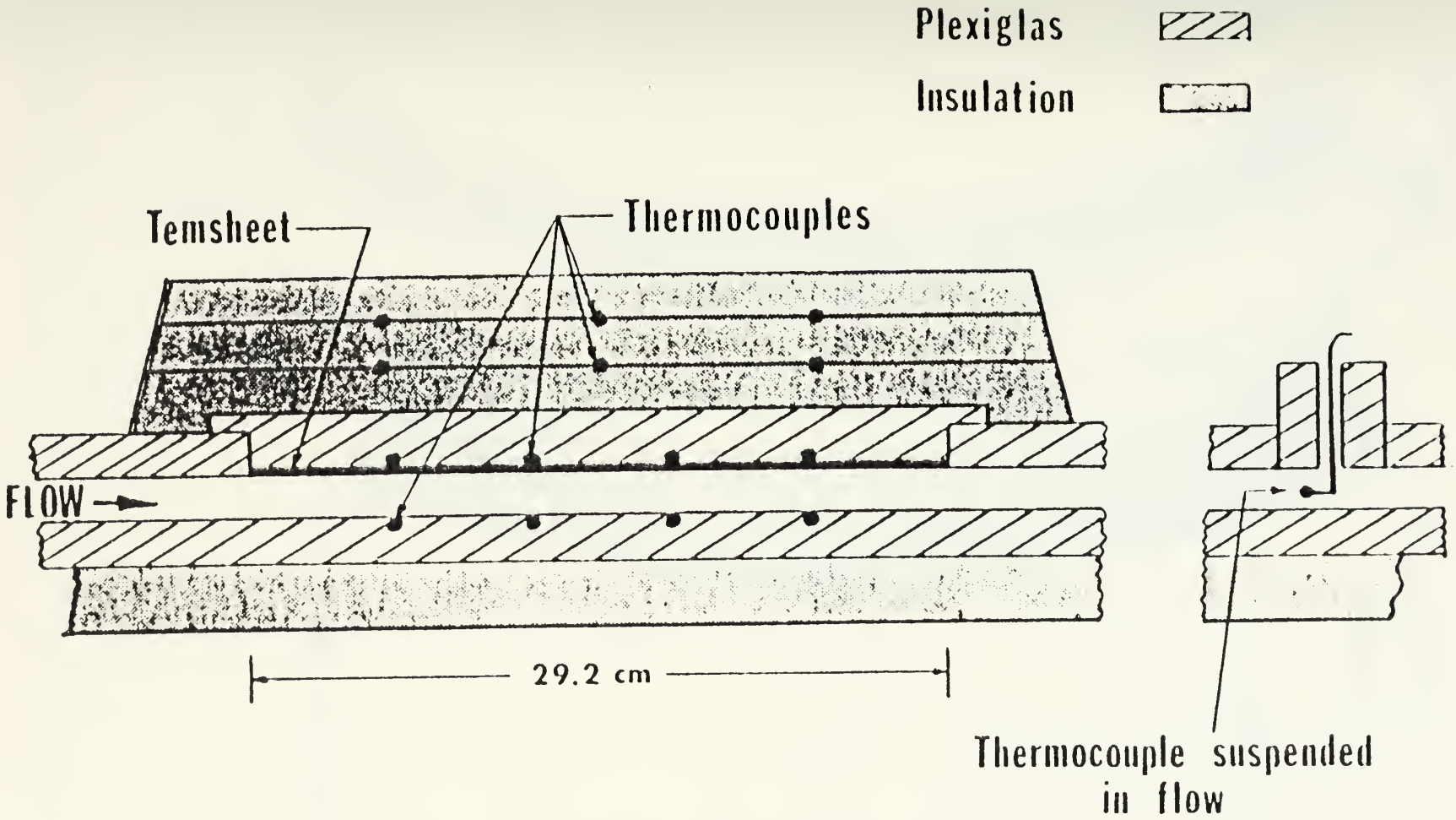

Figure 5. Straight test section, detailed schematic.

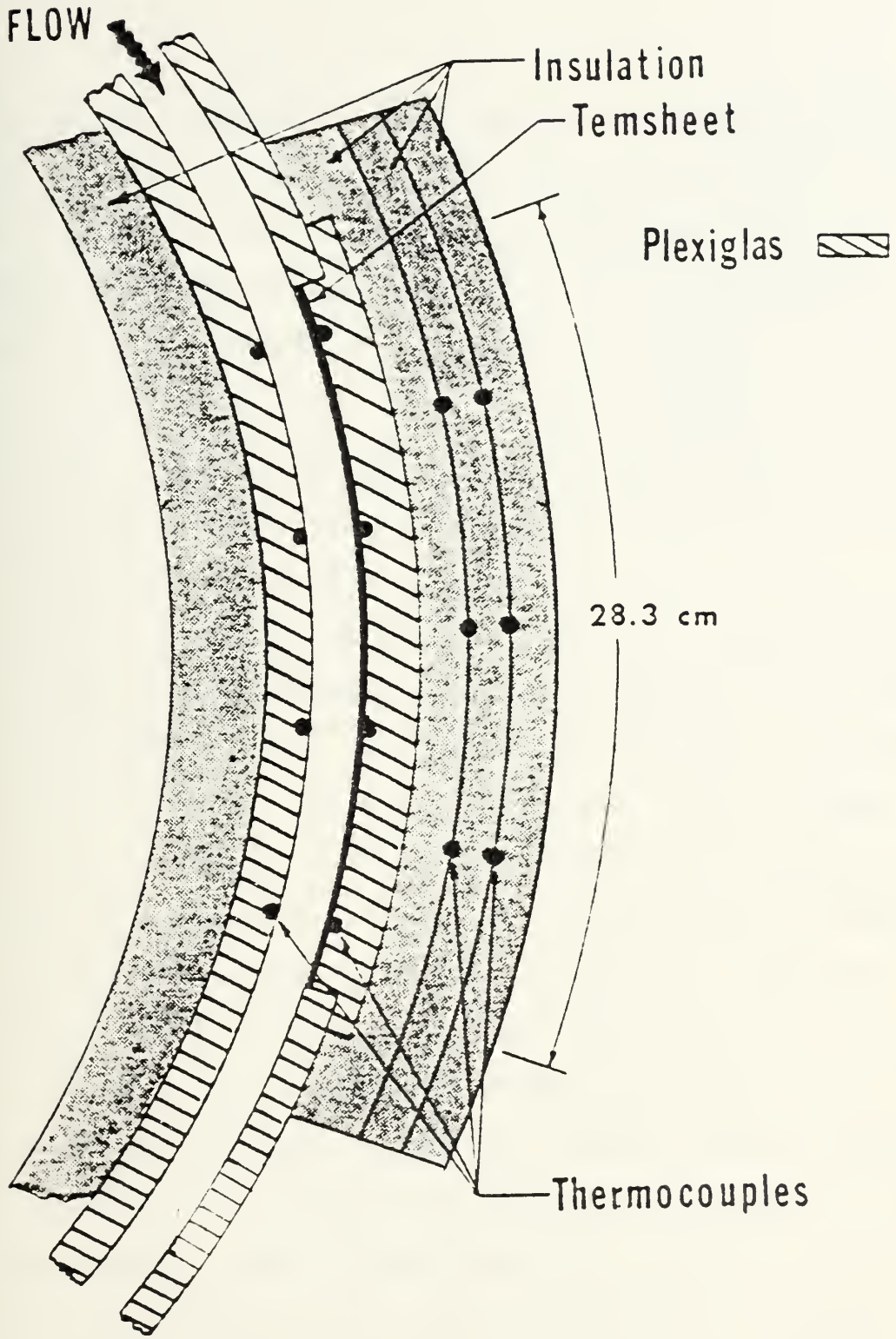

Figure 6. Curved test section, detailed schematic.

Each of the temperature measurements was made with Copper-Constantan thermocouples. Those thermocouples that could be removed easily from the channel were calibrated using a ROSEMONT Commutating Bridge model 920A, and a ROSEMONT Constant Temperature Bath model 913A. A second order polynomial was fitted to each set of data. The resulting coefficients differed by less than 1.0 percent, so an average of each coefficient was used in converting emf to degrees centigrade in the reduction of the data obtained.

A total of sixty-one Copper-Constantan, 30 gauge thermocouples were located throughout the test apparatus to record the desired temperatures. Four thermocouples were connected in parallel to read an average temperature at the entrance and exit to the channel. Five thermocouples were connected in parallel and inserted between each of the layers of insulation at each of the test sections. In addition, individual thermocouples were positioned in each of the test sections, eight in direct contact with the Temsheet and eight in the plexiglas of the unheated inner wall. Small diameter holes in the plexiglas were drilled to allow the installation of the thermocouples. One thermocouple was inserted in the two inch pvc pipe downstream of the orifice in accordance with the ASME Power Test Code to record the temperature of the air flowing through the orifice. The beads of the thermocouples in contact with the Temsheet were electrically insulated from the Temsheet with ENMAR Heat Resisting Glyceryl Phthalate.

The thermal insulation consisted of 1/4 inch layers of Armstrong Armaflex 22 Sheet Insulation, a flexible foamed plastic material, on the heated side of each test section, and 1/2 inch Armaflex 22 insulation elsewhere on the test apparatus. Three layers of the 1/4 inch insulation were used and covered an area slightly larger than each of the heated areas. By positioning thermocouples between these insulation layers, the heat lost to the environment could be computed at each test section. The heat loss through the 1/2 inch insulation surrounding the rest of the channel due to the heated air flowing through the channel was small in comparison. See Figure 7 for a detailed sketch of the thermocouple placement and attachment. The insulation was held in place by the use of Adhesive Heat Resistant ventilation Duct Tape. The entire channel and all connections between the channel, the pvc piping, and the orifice were sealed with General Electrical Silicone Rubber Sealant Caulk to ensure there was no leakage of air into the channel or the piping which could affect the temperatures recorded as well as the mass flow rate. Two aluminum electrodes, 0.318 centimeters thick, were inserted in between the Temsheet and the plexiglas in each section as shown in Figure 7.

The data acquisition system used for this investigation was a Hewlett Packard 3054A Automatic Data Acquisition/Control System consisting of a 3456A Digital Voltmeter and a 3497A Data Acquisition/Control Unit. Also used in conjunction with

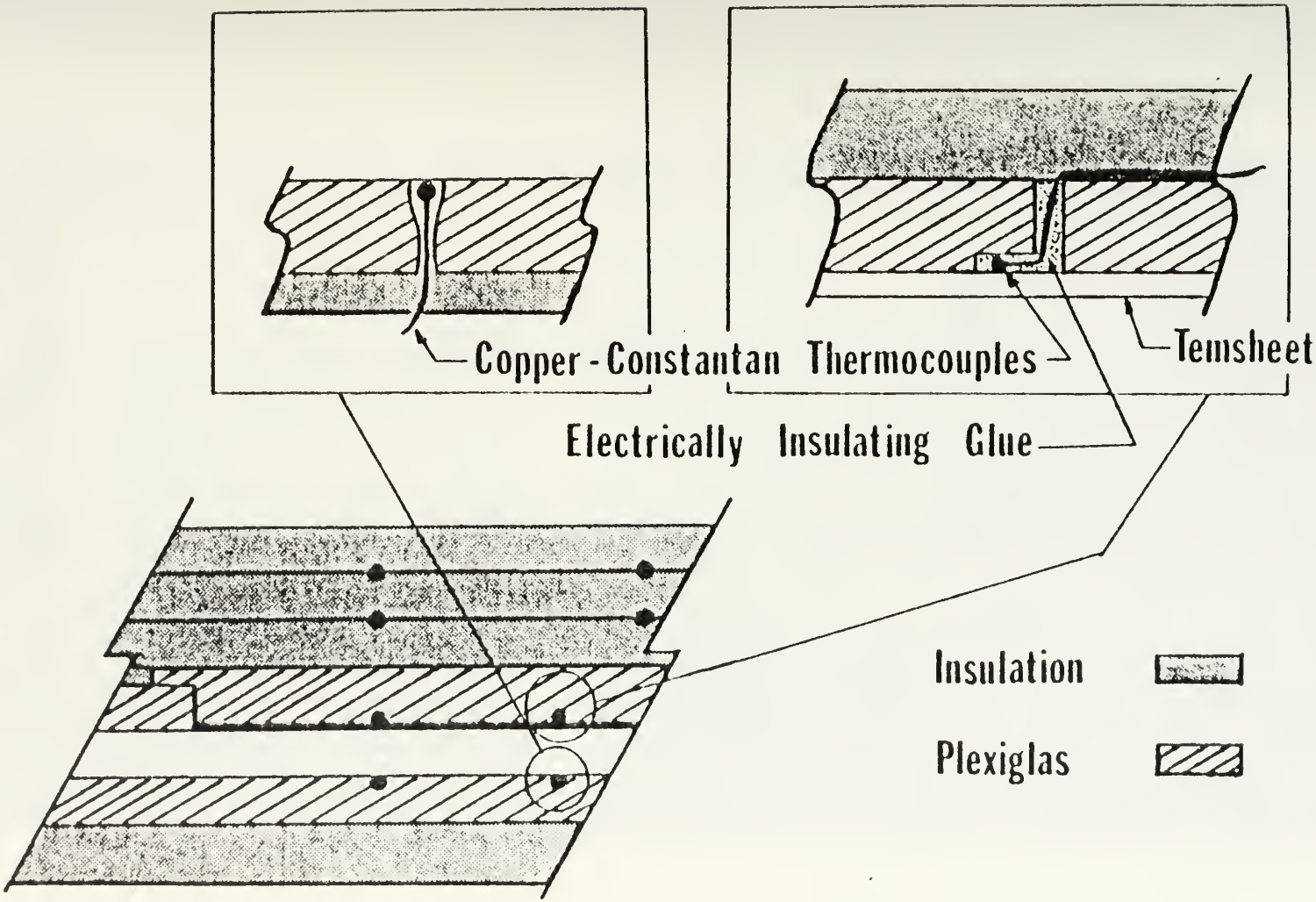

Figure 7. Thermocouple placement in test sections.

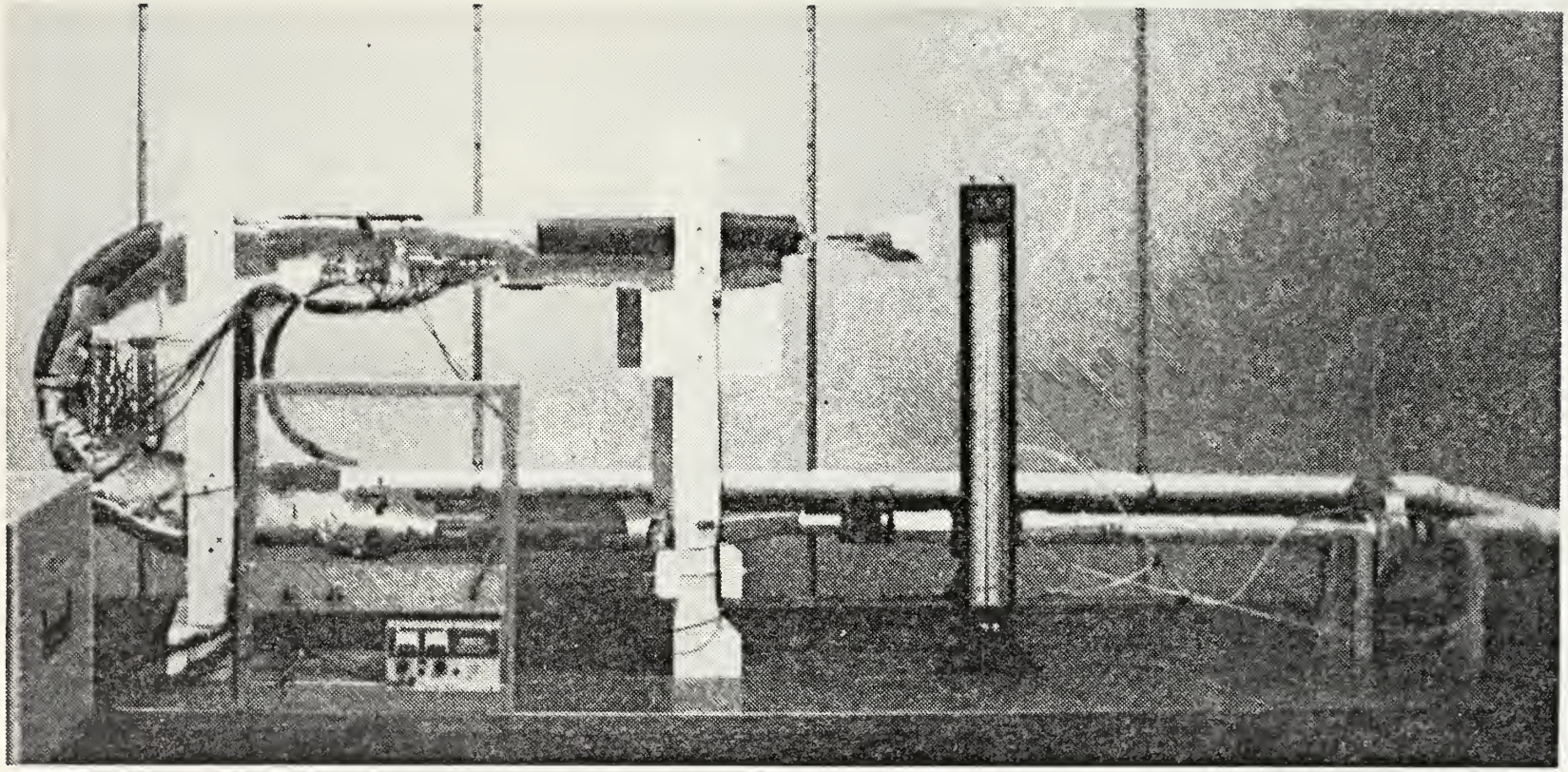

Figure 8. Photograph of test channel.

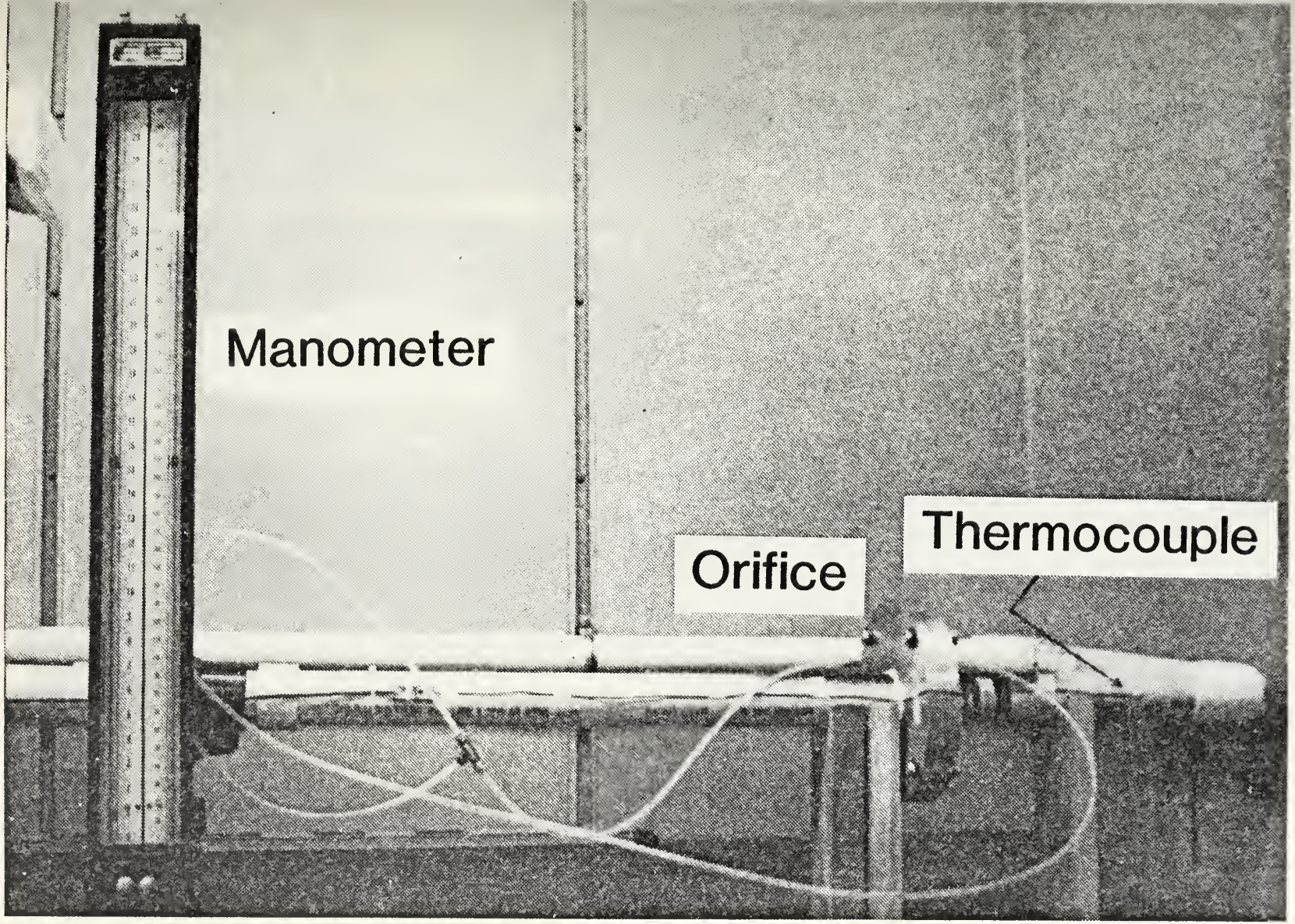

Figure 9. Photograph of flow measuring apparatus.

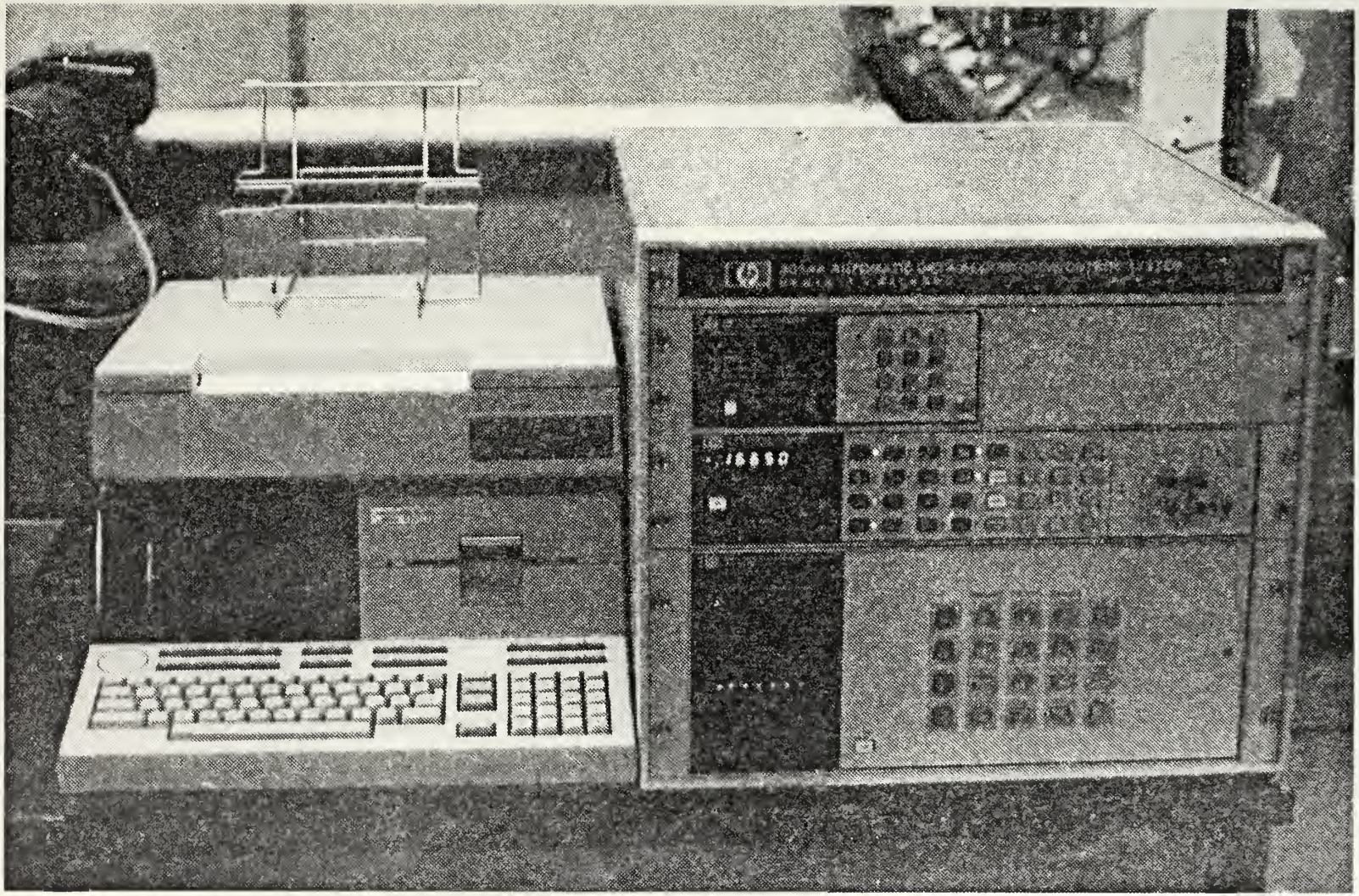

Figure 10. Photograph of data acquisition system.

this data acquisition system, were a Hewlett Packard 9326 Computer terminal and 2671G Printer. Pressure measurements were taken from Meriam vertical manometers, one whose fluid was water with a 0 to 60 inch range, and the other whose fluid was mercury, calibrated to read inches of water with a range of 0 to 415 inches. A photograph of the channel and associated test equipment are shown in Figures 8, 9, and 10.

B. EXPERIMENTAL PROCEDURES

Experiments were conducted by varying the mass flow rate of air corresponding to Reynolds numbers from approximately 12000 to 23000, where the Reynolds numbers are based on hydraulic diameter. For each mass flow rate, data was taken automatically by the data acquisition system and the data was immediately reduced and printed for examination and comparison. The experimental procedures followed were the same for the straight and curved test sections. The results obtained from the straight test section served as a baseline for the comparison of the curved section results. Preliminary runs were performed to determine the time required for the test rig to come to steady state. For this experiment three hours were allowed for steady state to be reached. After three hours, data was taken at ten minute intervals to observe changes in parameters to ensure that a steady state condition had been achieved. The criteria for steady state was based on three variables:

(1) the mass flow rate

(2) the heated boundary wall temperature

(3) the heater voltage

When these variables varied by less than two percent over a ten minute interval, it was considered that a steady state condition had been achieved.

It was also necessary to determine the approximate power setting required to bring the heated wall of each test section to approximately 50 degrees Centigrade. It had been determined by Holihan [Ref. 24] that this temperature was sufficient to ensure a 20 degree Centigrade difference in the heated wall and the unheated wall.

For each run, the atmospheric pressure, the pressure difference across the orifice, and the pressure upstream of the orifice were entered into the computer for the mass flow rate calculations. All other data was acquired by the data acquisition system directly from the experimental apparatus.

To compute the instantaneous power supplied the following relationship was used:

$$Q_P = \frac{V_H \, V_R}{R_{PR}}$$

The precision resistor voltage and the heater voltage were read by the data acquisition system and the resistance of the precision resistor was a known constant. A diagram of this circuit is shown in Figure 11.

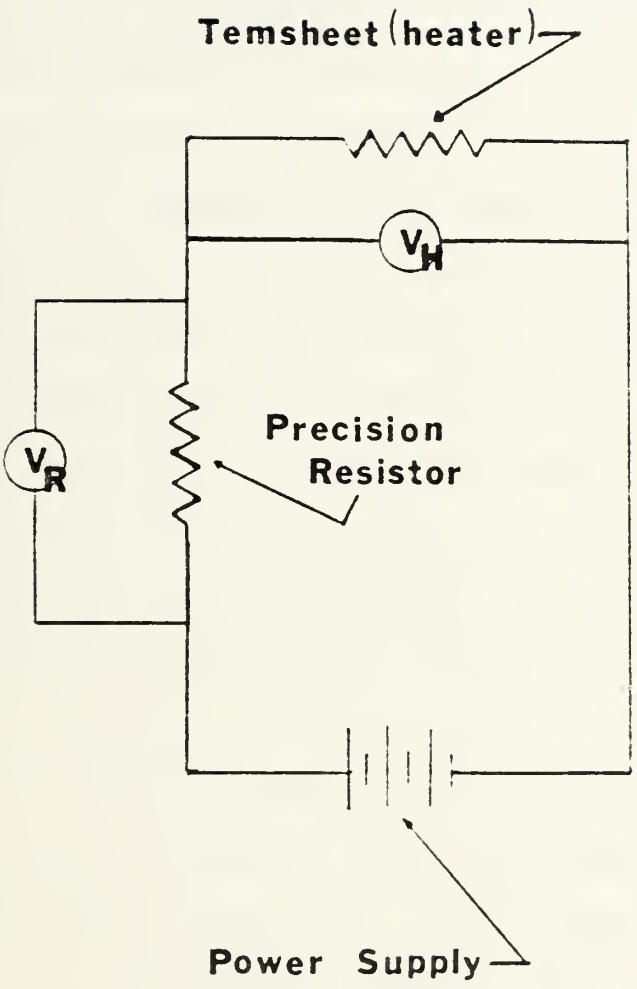

Figure 11. Circuit used to measure power supplied to the Temsheet.

IV. PRESENTATION OF DATA

A. ANALYSIS

The constant heat flux surface for the heated wall of each test section was approximated by the uniform electrical resistivity of the Temsheet. The insulated unheated wall was considered adiabatic since the heat losses through that wall were negligible. The channel's large aspect ratio of 40 allowed the modeling of the channel as parallel plates. The straight portion of the channel upstream of the straight test section was of sufficient length to ensure that the flow was hydrodynamically developed for the flow velocities of this study. The straight portion of the channel downstream of the curved test section was also of sufficient length to ensure that the flow exiting the channel was thoroughly mixed and that the temperature, T_{out}, was an average bulk temperature.

Based on these assumptions, the experimental configuration was modeled as forced convection between parallel plates, for hydrodynamically developed and thermally developing flows, subjected to a constant heat flux. The boundary conditions are one wall at a constant heat flux and the other wall insulated.

To analyze this problem, several quantities were defined as follows:

The heat convected to the air was calculated using the expression:

$$Q_{air} = \dot{m}\, C_p\, (T_{out} - T_{in})$$

where 'C_{pair}' was the specific heat of the air at constant pressure and '$\dot{m}$' was the mass flow rate of the air.

The average heat transfer coefficient between the heated wall and the flow of air in the channel was defined by the equation:

$$\bar{h} = \frac{Q_{air}}{A_{PL}\ \Delta T}$$

where 'Q_{air}' is defined above, 'A_{PL}' was the area of the Temsheet in the test section, and 'ΔT' was the difference between the average heated wall temperature (T_{wo}) and the average bulk temperature (T_{blk}). The average bulk temperature was defined as the arithmetic mean of the entrance and exit temperatures (T_{in}, T_{out}).

The average Nusselt number was then calculated as follows:

$$\overline{Nu} = \frac{\bar{h}\ D_{hd}}{K_{air}}$$

In this equation 'D_{hd}' is the hydraulic diameter and 'K_{air}' is the thermal conductivity of air.

The Reynolds number was calculated for each test run as follows:

$$Re_{hd} = \frac{\dot{m}\ D_{hd}}{A_c\ \mu_{air}}$$

where again '$\dot{m}$' and 'D_{hd}' are the mass flow rate and hydraulic diameter of the channel, 'A_c' is the cross-section of the channel, and 'μ_{air}' is the dynamic viscosity of the air.

For the curved section runs a Dean number was defined as:

$$De = Re_{hd} \sqrt{\frac{D_{hd}}{Ri}}$$

where 'Re' is the Reynolds number based on hydraulic diameter, 'D_{hd}' is the hydraulic diameter, the 'Ri' is the radius of curvature of the unheated inner convex wall.

A sketch of the control volume and a set of sample calculations for one test run of the curved section are given in Appendix B.

B. RESULTS

The data obtained from each experimental run was evaluated utilizing the expressions described in Part A above. The major parameters resulting from this evaluation are shown in Tables I and II. Table I contains the straight section results and Table II contains the results of the curved section. A plot of the average Nusselt number verses Reynolds number is given in Figure 12 for the comparison of the results. Error bands have been indicated as a result of an uncertainty analysis. A sample calculation for the uncertainty analysis is given in Appendix A.

The results indicate an increase in the rate of heat transfer with increasing Reynolds number for both the

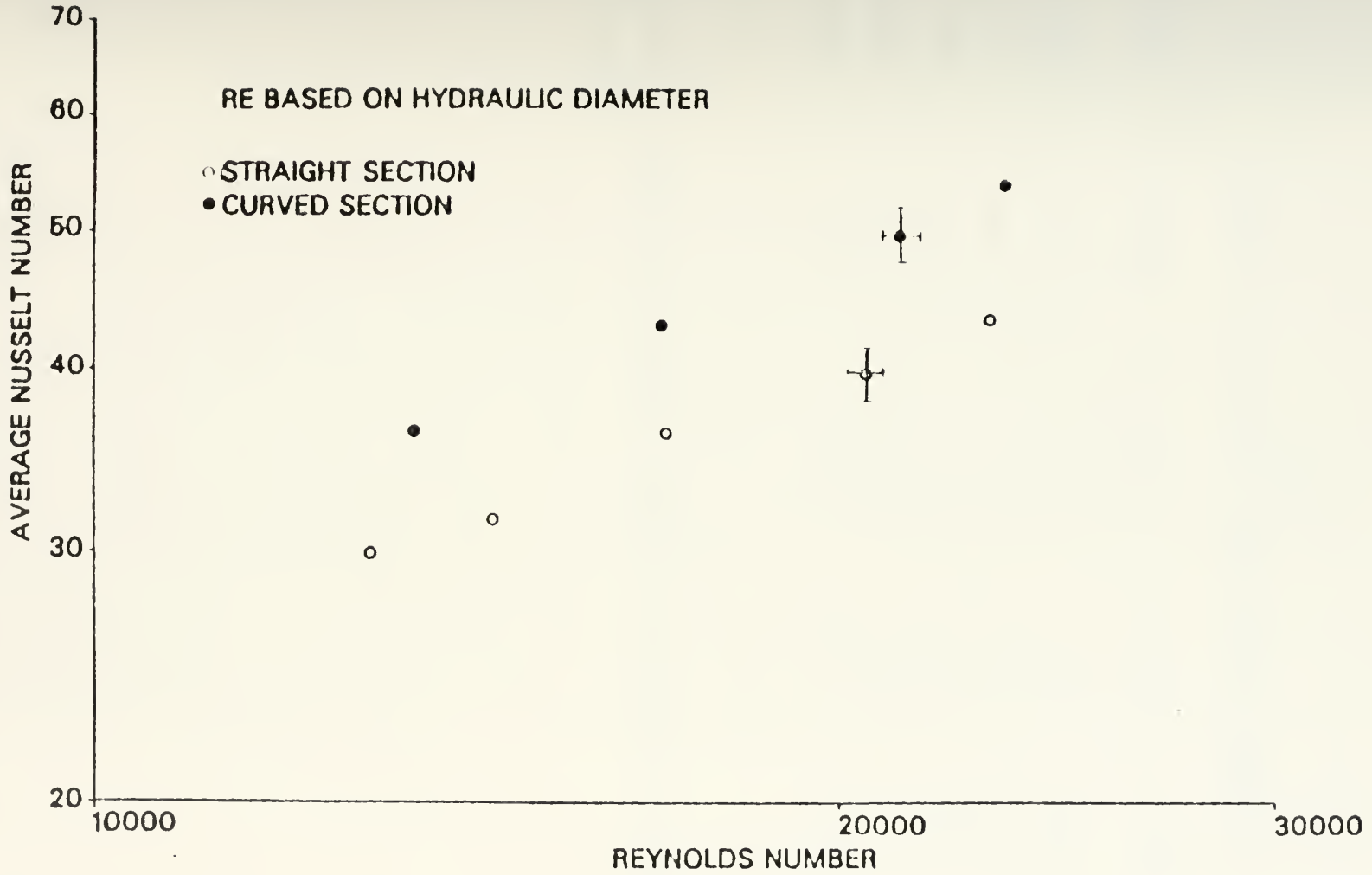

Figure 12. Straight vs. curved section results, present study.

TABLE I

SUMMARY OF STRAIGHT TEST SECTION RESULTS

Re_{hd}	Q_{air} (W)	$\bar{h}$ (W/m C)	ΔT (C)	$\overline{Nu}$
12940	114.43	63.55	24.27	29.9
14520	113.55	67.05	22.82	31.5
17020	120.00	76.70	21.09	36.1
20480	117.37	84.30	18.76	39.7
22980	121.31	92.04	17.76	43.4

Reynolds number and Nusselt number are based on hydraulic diameter.

TABLE II

SUMMARY OF CURVED TEST SECTION RESULTS

Re_{hd}	De	Q_{air} (W)	$\bar{h}$ (W/m C)	ΔT (C)	$\overline{Nu}$
13490	2707	115.28	77.23	20.79	36.2
16950	3403	117.50	91.26	17.93	42.9
21140	4243	114.94	105.46	15.18	49.7
23320	4680	113.43	111.47	14.17	53.9

Reynolds number, Dean number, and Nusselt number are based on hydraulic diameter.

straight and curved test sections. In addition, the heat transfer rate was higher for each Reynolds number investigated in the curved section.

In the investigation by Holihan [Ref. 24] a straight line least squares correlation of his data resulted in:

$$\overline{Nu} = 0.983\ Re_d^{0.25} \qquad 300 < Re_d < 2000$$

for laminar flows, and

$$\overline{Nu} = 0.110\ Re_d^{0.56} \qquad 2000 < Re_d < 3000$$

for transition flows in the straight test section. The curved section data yielded:

$$\overline{Nu} = 0.065\ Re_d^{0.67} \qquad 300 < Re_d < 2000$$

for laminar flow, and

$$\overline{Nu} = 0.117\ Re_d^{0.58} \qquad 2000 < Re_d < 3000$$

for transition flows.

The data for the present study resulted in

$$\overline{Nu} = 0.063\ Re_{hd}^{0.65} \qquad 10^4 < Re_{hd} < 2.5 \times 10^4$$

for turbulent flow in the straight test section, and

$$\overline{Nu} = 0.040\ Re_{hd}^{0.72} \qquad 10^4 < Re_{hd} < 2.5 \times 10^4$$

for similar flow in the curved section.

In the turbulent regime of this study, the rate of heat transfer was about twenty percent higher in the curved section when compared with the straight section. This compares favorably with earlier studies by Kreith [Ref. 16], where he reported an increase in the rate of heat transfer along a concave wall of from twenty-five to sixty percent for Reynolds numbers, based on hydraulic diameter, between 10^4 and 10^6. Holihan reported an increase of fifteen percent for laminar flow and thirty percent for transition flow [Ref. 24]. Ballard reported an increase of eleven percent in the heat transfer rate for laminar flows [Ref. 23].

V. DISCUSSION AND CONCLUSIONS

Holihan [Ref. 24], in his study, determined that there was a negligible difference in the fluid bulk temperature and the unheated wall temperature. He additionally demonstrated that the radiated heat transfer from the unheated wall surface was minimal. These results were verified for the present study and provide the basis for the assumption that the heat transfer to the air flowing through the channel was solely by convection from the heated Temsheet.

As was mentioned earlier, the high aspect ratio of the channel provided the basis for the assumption that the experimental apparatus, as configured, could be modeled as infinite parallel plates. Holihan's data [Ref. 24] also tended to verify this assumption. His experimental data, in the laminar flow region, approached the theoretical limit for average Nusselt number for parallel plates with one wall heated at a constant heat flux and the opposite wall adiabatic [Ref. 27].

Based on the assumptions mentioned above, comparisons were made with other analytical and experimental results that were of the same or similar problem. Again the problem being, flow between infinite parallel plates with one wall at a constant heat flux and the opposite wall adiabatic.

A comparison of the experimental results of this study and the experimental results of Ballard [Ref. 23] and Holihan [Ref. 24] are shown in Figure 13, for the straight section, and Figure 14 for the curved section. Figure 15 shows a compilation of all the data on one plot. Ballard's data was strictly in the laminar region, while Holihan's data covered the laminar as well as transition regions. The channel aspect ratio was 40 for each of these studies and the experimental procedures were similar in each case. Ballard and Holihan compared their data to the analytical studies by McCuen, [Ref. 28], for heat transfer between infinite parallel plates with constant wall temperatures and heat flux. Their results plotted above the analytical solution and the difference was attributed to the difference in the geometries used in the studies, and to the limitations inherent in any experimental work. The side wall effects and the inability to totally account for all the heat transfer processes and/or losses were also factors that may have caused the difference.

A comparison of analytical and experimental results with those of the present study for the straight test section is shown graphically in Figure 16. The results of Shibani and Ozisik [Ref. 19] is shown for turbulent flow between parallel plates. The correlation used was

$$Nu = 12 + .024\ Re^{.824}$$

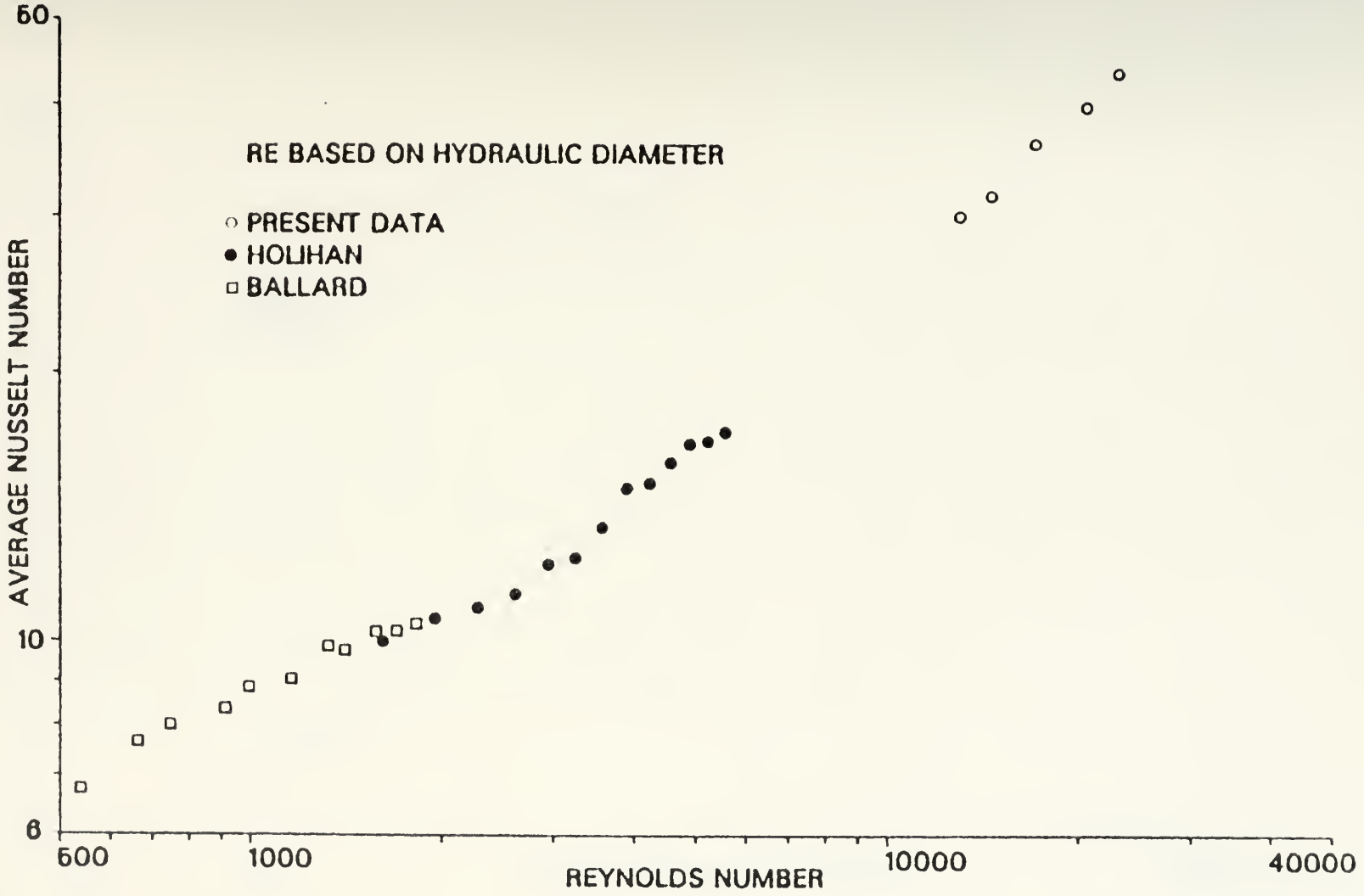

Figure 13. Comparison of present data with Ballard and Holihan, straight section.

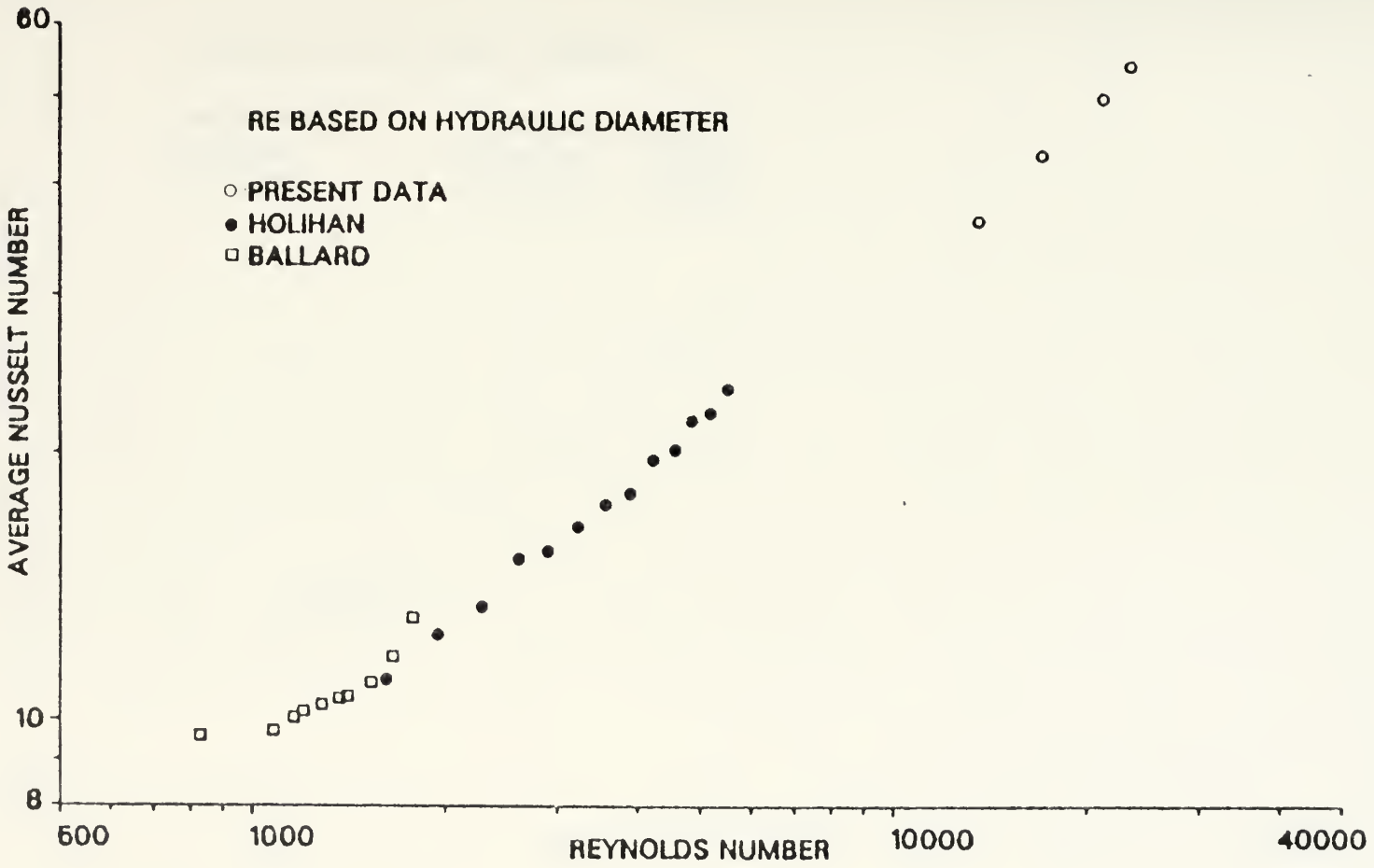

Figure 14. Comparison of present data with Ballard and Holihan, curved section.

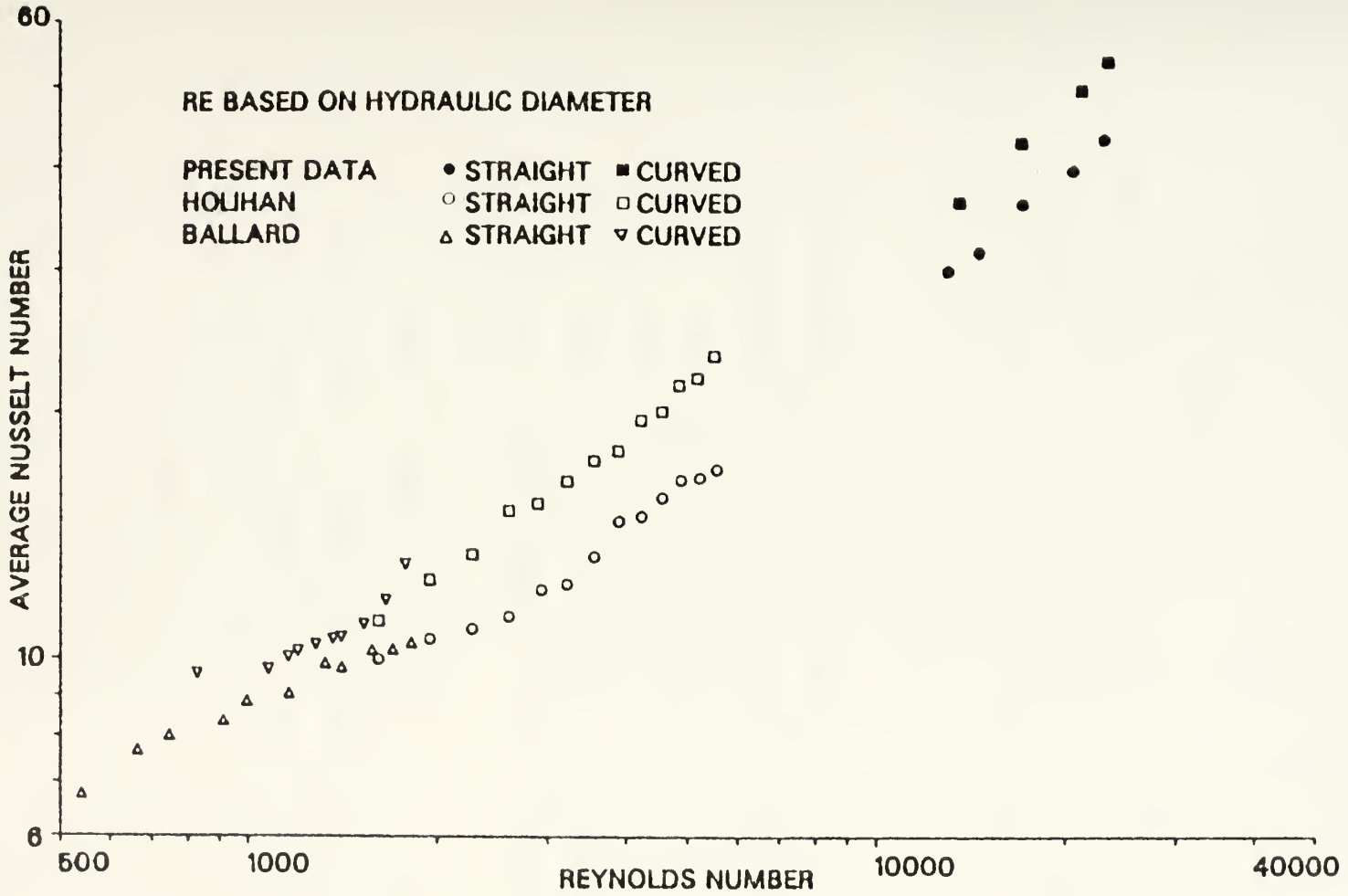

Figure 15. Comparison of present data with Ballard and Holihan, straight and curved section.

for $0.1 < Pr < 10$ and $10^4 < Re < 10^6$. The Dittus-Boelter equation [Ref. 26] for heat transfer in a straight tube for constant wall temperature is plotted from the following correlation:

$$Nu = .02\ Re^{.8}$$

for a Prandtl number equal to 0.71. Additionally, Kays and Leung [Ref. 21] obtained data for heat transfer in annular passages, with one wall heated at a constant heat rate. The data shown is for $r^* = 1.0$ which equates to parallel plates.

The curve section data is plotted in Figure 17 and is compared with the experimental results of Brinich and Graham [Ref. 25] for flow and heat transfer in a curved channel. The accuracy of the data points used are subject to errors, in that the actual values were not given in their study and had to be taken from a plot of Stanton number versus Reynolds number as given in the reference.

The data from the present study fell below the correlations that were used as comparisons. These differences can also be attributed to the differences in geometries and conditions of heating used. Experimental error and side wall effects may have also contributed to the overall difference in results.

The data from the present study and that from the Brinich and Graham study seem to compare favorably and exhibit a similar trend. Irrespective of the differences noted above, it

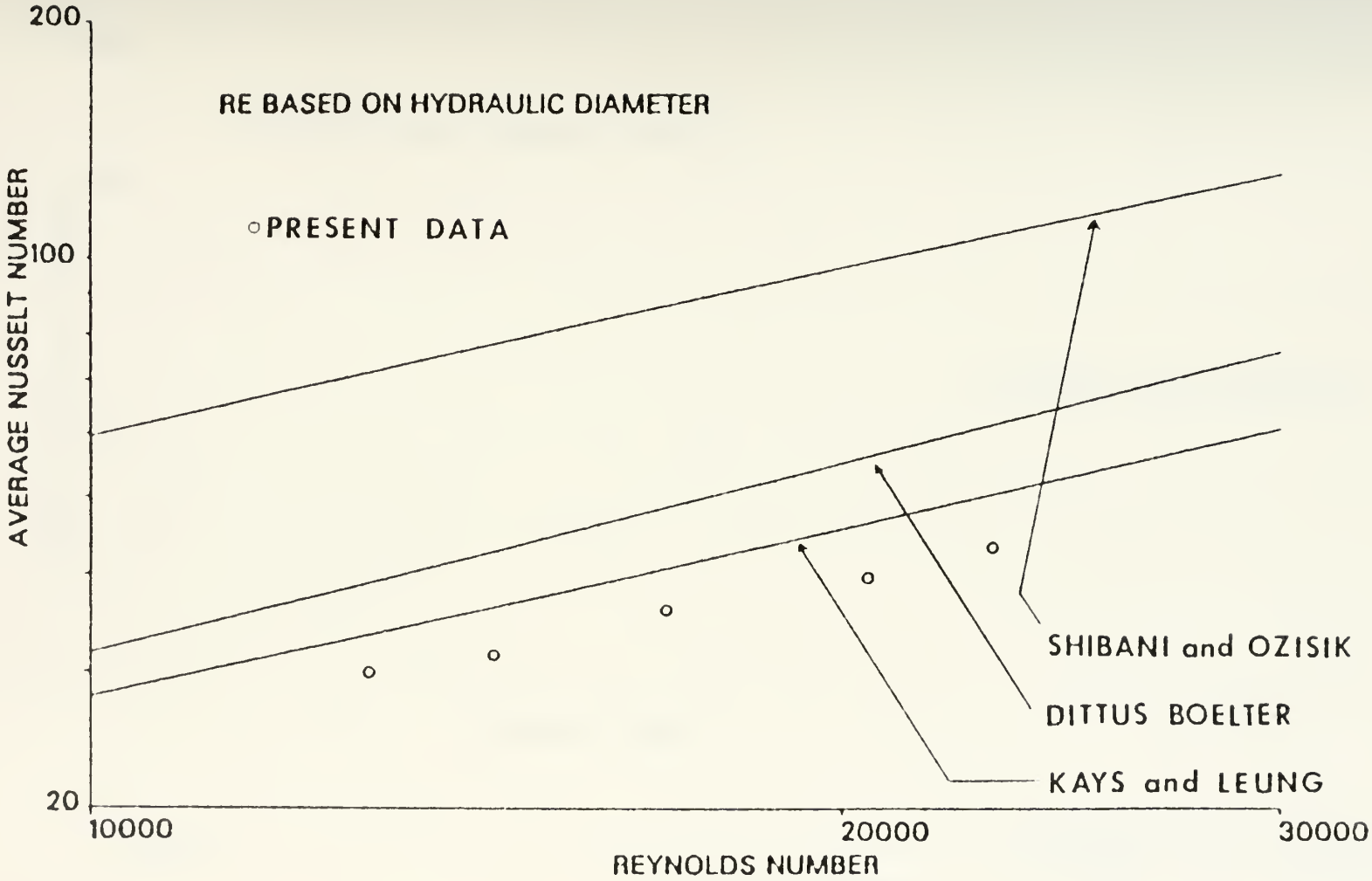

Figure 16. Comparison of present data with Shibani and Ozisik, Dittus-Boelter, Kays and Leung, for turbulent flow, straight section.

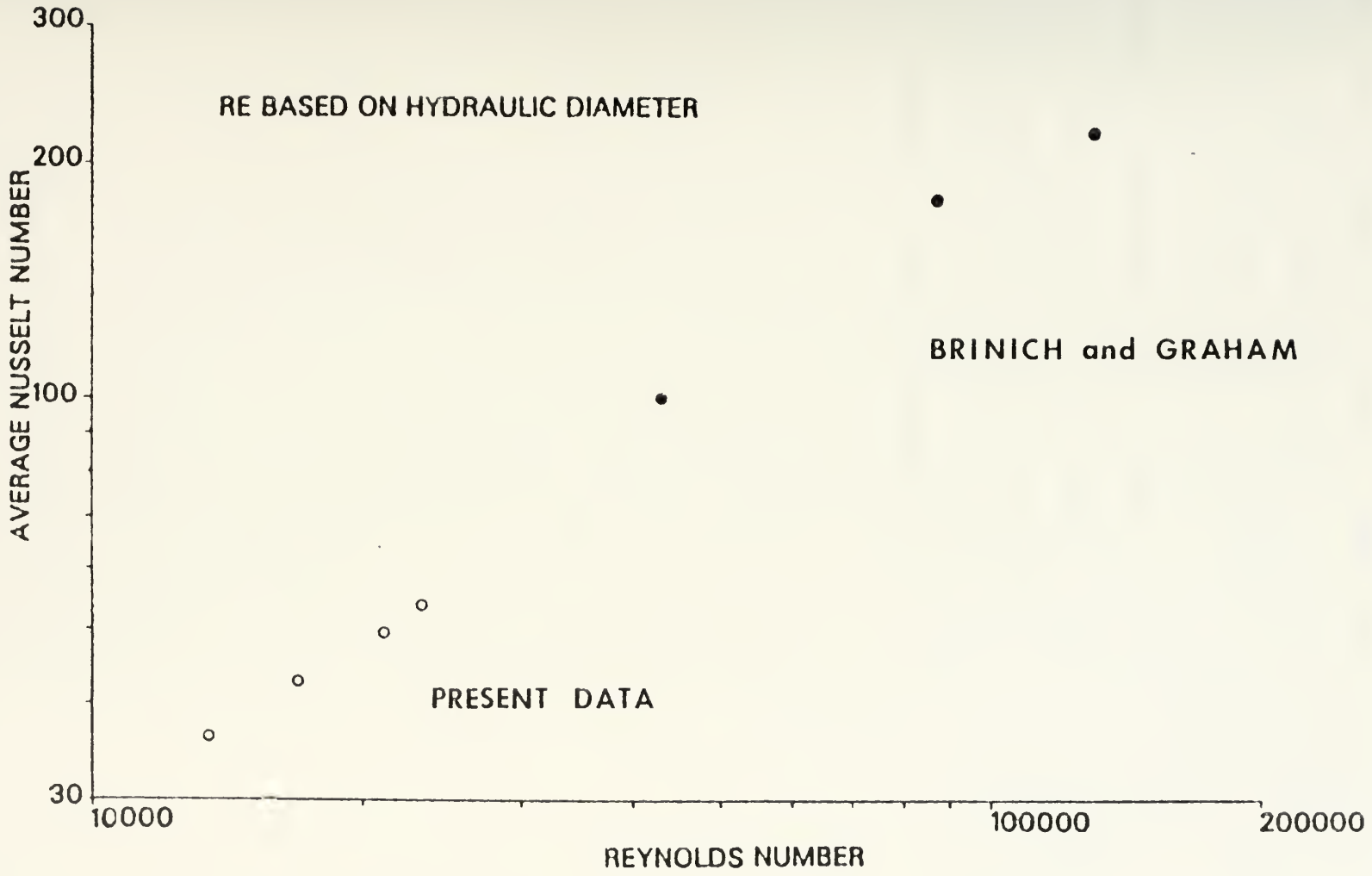

Figure 17. Comparison of present data with Brinich and Graham, for turbulent flow, curved section.

appears that there is a definite enhancement of the heat transfer rate in the curved test section for laminar, transition, and turbulent flows. Streamwise curvature, resulting in secondary flows, seems to cause the enhancement. Whether the Taylor-Gortler vortices continue into the transition and turbulent flow regimes remains to be seen. Continued study of the effect of streamwise curvature and the development and propagation of the Taylor-Gortler vortices throughout all flow regimes is required.

VI. RECOMMENDATIONS

To better understand the effects of streamwise curvature on the enhancement of heat transfer, a significant amount of study still remains. With the introduction of today's data acquisition systems, in conjunction with portable computers, instantaneous recording of data and its reduction, for immediate analysis, saves an immeasurable amount of time and reduces the chance of human error. The present experimental apparatus has been used over a range of Reynolds numbers throughout the laminar and transition regimes, into the turbulent regime. Results have compared well with previous data and correlations. A new flow channel of similar design should be constructed prior to further testing, due to the age and condition of the present equipment. A new set of calibrated thermocouples and possibly the introduction of pressure transducers, instead of manometers, that could be connected to the data acquisition system, would provide more consistent, and as a result, more accurate data for flow rate measurements. Also, since the present apparatus has been modified several times in the past, resulting in leaks that are difficult to locate and stop, a new flow channel would help to eliminate some of the inaccuracies to temperature and flow measurements introduced by undiscovered leaks. It is also highly recommended that a method of safeguarding each piece of equipment,

so that in the event of a power failure, when power is restored, each item would require the operator to manually restart it.

APPENDIX A: EXPERIMENTAL UNCERTAINTY

The uncertainties for the major variable in the experiments, were calculated in accordance with the method described by S. Kline and F. McClintoch [Ref. 29]. The estimates of the uncertainty in the measured quantities were made conservatively. As a result, there is considerable confidence in the uncertainties as calculated.

The following equations were used to calculate the uncertainties:

$$(1)\quad d\dot{m} = \dot{m}\left[YKA\left(\frac{dY}{Y}\right)^2 + \left(\frac{dK}{K}\right)^2 + \left(\frac{dA}{A}\right)^2\right)^{1/2} + \left(1/2\ \rho_{air}\Delta P\left(\left(\frac{d\rho_{air}}{\rho_{air}}\right)^2 + \left(\frac{d\Delta P}{\Delta P}\right)^2\right)^{1/2}\right]^{1/2}$$

$$(2)\quad dQ_{air} = Q_{air}\left(\left(\frac{d\dot{m}}{\dot{m}}\right)^2 + \left(\frac{d\ C_{pair}}{C_{pair}}\right)^2 + \left(\frac{d(T_{out}-T_{in})}{T_{out}-T_{in}}\right)^2\right)^{1/2}$$

$$(3)\quad d\bar{h} = \bar{h}\left(\left(\frac{dQ_{air}}{Q_{air}}\right)^2 + \left(\frac{dA_{PL}}{A_{PL}}\right)^2 + \left(\frac{d\Delta T}{\Delta T}\right)^2\right)^{1/2}$$

$$(4)\quad d\overline{Nu} = \overline{Nu}\left(\left(\frac{d\bar{h}}{\bar{h}}\right)^2 + \left(\frac{dD_{hd}}{D_{hd}}\right)^2 + \left(\frac{dK_{air}}{K_{air}}\right)^2\right)^{1/2}$$

$$(5)\quad dRe_{hd} = Re_{hd}\left(\left(\frac{d\dot{m}}{\dot{m}}\right)^2 + \left(\frac{dD_{hd}}{D_{hd}}\right)^2 + \left(\frac{d\mu_{air}}{\mu_{air}}\right)^2 + \left(\frac{dA_c}{A_c}\right)^2\right)^{1/2}$$

The values obtained for the uncertainties for the values in the curved section test run at a Reynolds number of 17500 are:

Quantity	Uncertainty
A	.0005
A_{PL}	.0026
A_c	.0098
C_p	.0034
D_{hd}	.0087
$\bar{h}$	.0412
K	.0050
K_{air}	.0012
$\overline{Nu}$	.0421
$\dot{m}$	.0223
Q_{air}	.0382
Re_{hd}	.0260
T_{blk}	.0092
T_{in}	.0046
T_{out}	.0049
T_{wo}	.0063
$T_{out}-T_{in}$	.0136
Y	.0051
ΔP	.0222
ΔT	.0032
μ_{air}	.0027
ρ_{air}	.0003

The major source of uncertainty in the average Nusselt number is the uncertainty in the pressure readings from the manometer which affects the mass flow rate calculation. In order to obtain a more accurate pressure measurement, it has been recommended that pressure transducers or inclined manometers be used instead of vertical manometers in future studies.

APPENDIX B: SAMPLE CALCULATIONS

Figure 18 below, shows the major heat transfer components for each of the test sections. The sample calculations that follow, demonstrate the methods used by the computer to calculate these components as well as the Reynold's number, average heat transfer coefficient, and average Nusselt number for each set of data. The sample calculations are for the curved section, but those for the straight section are similar. Reynolds number, Nusselt number, and Dean number are based on hydraulic diameter.

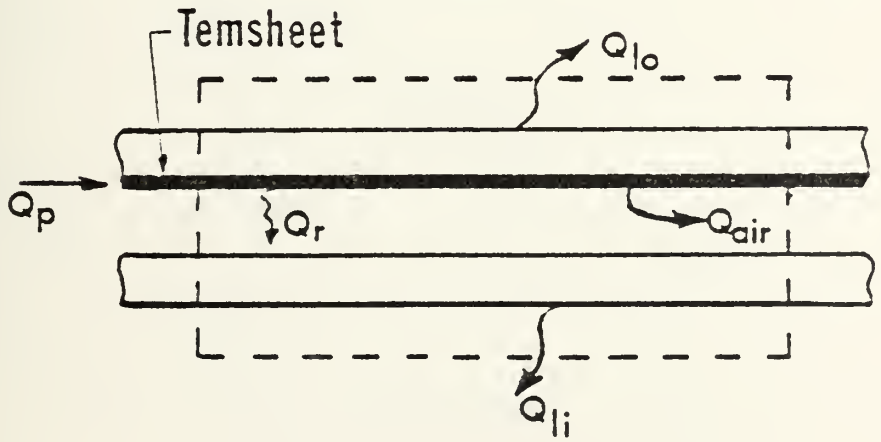

Figure 18. Energy balance in straight section.

A. SAMPLE CALCULATION DATA

V_H = 55.2325 V

V_R = 4.4075 V

R_{PR} = 2.0262 Ω

P_{atm} = 30.45 in. Hg

ΔP = 22.5 in. H_2O

P_1 = 13.05 in. H_2O

T_{in} = 25.41 C

T_{out} = 28.08 C

T_{wo} = 44.50 C

T_{wi} = 25.99 C

T_{ins1} = 38.66 C

T_{ins2} = 32.52 C

T_{orif} = 28.32 C

K_{air} = 26.52×10^{-3} W/mK

C_{pair} = 1006 J/Kg K

μ_{air} = 18.63×10^{-6} Kg/ms

K_{ins} = 3.6495×10^{-2} W/mK

ΔX_{ins} = 0.00635 m

ε_{wo} = 0.70

ε_{wi} = 0.40

σ = 5.669×10^{-8} W/m^2K^4

β = .5325

γ = 1.402

gc = 1 Kg m/NS^2

R = 286.8 Nm/Kg K

F_{wo-wi} = 1.0

A_{PL} = .07188 m^2

A_c = .0016 m^2

A_{pipe} = .002027 m^2

D_c = .00635 m

D_{pipe} = .0508 m

D_{orif} = .027051 m

P_{wet} = .5207 m

B. TEMPERATURE CALCULATIONS

1. Bulk Temperature (T_{blk})

$$T_{blk} = \frac{T_{in} + T_{out}}{2} = \frac{25.41 + 28.08}{2} = 26.75 \text{ C}$$

2. Mean Temperature Difference (ΔT)

$$\Delta T = T_{wo} - T_{blk} = 44.50 - 26.75 = 17.75 \text{ C}$$

3. Temperature Difference in the Insulation (ΔT_{ins})

$$\Delta T_{ins} = T_{ins1} - T_{ins2} = 38.66 - 32.52 = 6.14 \text{ C}$$

C. POWER CALCULATIONS

1. Power Supplied (Q_p)

$$Q_p = \frac{V_H\ V_R}{R_{PR}} = \frac{(55.2325)(4.4075)}{(2.0262)} = 120.14\ W$$

2. Heat Lost Through the Outer Plate (Q_{lo})

$$Q_{lo} = \frac{\Delta T_{ins}}{(\Delta X_{ins})/(K_{ins})(A_{PL})} = \frac{6.14}{(0.00635)/(3.6495\text{x}10^{-2})(.07188)}$$

$$= 2.54\ W$$

3. Heat Radiated (Q_r)

a. Radiation Resistance (R_R)

$$R_R = \frac{1\ -\varepsilon_{wo}}{A_{PL}\varepsilon_{wo}} + \frac{1}{A_{PL}\ F_{wo-wi}} + \frac{1\ -\varepsilon_{wi}}{A_{PL}\varepsilon_{wi}}$$

$$= \frac{1}{A_{PL}}\left[\frac{1}{\varepsilon_{wo}} + \frac{1}{\varepsilon_{wi}} - 1\right] = \frac{1}{(0.07188)}\left[\frac{1}{0.7}+\frac{1}{0.4}-1\right] = 40.74\ m^{-2}$$

b. Heat Radiated (Q_r)

$$Q_r = \frac{\sigma(T_{wo}^{\ 4} - T_{wi}^{\ 4})}{R_R} \qquad T[=]K$$

$$= \frac{(5.669\text{x}10^{-8})[(44.50+273)^4 - (25.99+273)^4]}{40.74}$$

$$= 3.02\ W$$

D. MASS FLOW RATE CALCULATIONS

1. Pressure Conversions

a. P_{atm}=30.45 in Hg x 3374.1 = 102741.35 N/m^2

b. $\Delta P = 22.5 \text{ in } H_2O \times 248.64 = 5594.4 \text{ N/m}^2$

c. $P_1 = (13.05 \text{ in } H_2O \times 248.64) + 102741.35 = 105986.10 \text{ N/m}^2$

2. Density of Air (ρ_{air})

$$\rho_{air} = \frac{P_{atm}}{R\,T_{orif}} = \frac{(102741.35)}{(286.8)(28.32+273)} = 1.1889 \text{ Kg/m}^3$$

3. Expansion Factor (Y)

$$Y = 1-[0.333+1.145(\beta^2+0.7\beta^5+12\beta^{13})]\,\frac{\Delta P}{\gamma P_1}$$

$$= 1-[0.333+1.145((.5325)^2+0.7(.5325)^5+12(.5325)^{13}] \times \frac{5594.4}{(1.402)(105986.10)}$$

$$= .9738$$

4. Area of Orifice (A)

$$A = \frac{\pi(D_{orif})^2}{4} = \frac{\pi(.02705)^2}{4} = .0005747 \text{ m}^2$$

5. Mass Flow Rate ($\dot{m}$)

$$\dot{m} = YKA\sqrt{2g_c\rho_{air}\Delta P} = (.9738)K(.0005747) \times \sqrt{2(1)(1.1889)(5594.4)}$$

$$\dot{m} = .06455\ K$$

Iterating:

Assume a Reynolds number $_{pipe}$ = 55000

Obtain a value for K, the flow coefficient, from reference 30. K = .6332

Solve for $\dot{m}$. $\dot{m}$ = .0409 Kg/s

Solve for new $Re_{pipe} = \frac{\dot{m} D_{pipe}}{A_{pipe} \mu_{air}} = \frac{(.0409)(.0508)}{(.002027)(18.63x10^{-6}}$

Re_{pipe} = 54988

Check convergence and repeat process if necessary.

(Convergence if difference less than .001)

$\dot{m}$ = .0409 Kg/s

E. REYNOLDS NUMBER CALCULATIONS

1. $Re_{pipe} = \frac{\dot{m} D_{pipe}}{A_{pipe} \mu_{air}} = \frac{(.0409)(.0508)}{(.002027)(18.63x10^{-6}} = 54988$

2. $Re_d = \frac{\dot{m} D_c}{A_c \mu_{air}} = \frac{(.0409)(.00635)}{(.0016)(18.63x10^{-6}} = 8713$

3. $Re_{hd} = \frac{\dot{m} D_{hd}}{A_c \mu_{air}}$

a. $D_{hd} = \frac{4 \times A_c}{P_{wet}} = \frac{(4)(.0016)}{.5207} = .01229$ m

$Re_{hd} = \frac{\dot{m} D_{hd}}{A_c \mu_{air}} = \frac{(.0409)(.01229)}{(.0016)(18.63x10^{-6}} = 16863$

F. HEAT CONVECTED TO AIR CALCULATION

1. $Q_{air} = \dot{m} C_p (T_{out} - T_{in}) = (.0409)(1006)(28.08-25.41) - 109.86W$

G. AVERAGE HEAT TRANSFER COEFFICIENT CALCULATION

$$\bar{h} = \frac{Q_{air}}{A_{PL}\ \Delta T} = \frac{109.86}{(.07188)(17.75)} = 86.11\ W/m^2C$$

H. AVERAGE NUSSELT NUMBER CALCULATION

$$\overline{Nu} = \frac{\bar{h}\ D_{hd}}{K_{air}} = \frac{(86.11)(.01229)}{26.52 \times 10^{-3}} = 39.90$$

I. DEAN NUMBER CALCULATION

$$De = Re_{hd}\sqrt{\frac{D_{hd}}{R_i}} = 16863\ \sqrt{\frac{.01229}{.305}} = 3385$$

APPENDIX C: CORRELATIONS

The correlations obtained for the present study were obtained using the method of least squares for a first degree polynomial, as outlined by C. F. Gerald [Ref. 29]. In this method the values of Reynolds number (x) and Nusselt number (Y) were first converted to their natural logarithmic value. Next the summations of x_i, x_i^2, Y_i, and x_iY_i were calculated. The values of these quantities were then placed in a matrix:

$$\begin{bmatrix} N & \Sigma x_i \\ \Sigma x_i & \Sigma x_i^2 \end{bmatrix} \begin{bmatrix} a_o \\ a_1 \end{bmatrix} = \begin{bmatrix} \Sigma Y_i \\ \Sigma x_i Y_i \end{bmatrix}$$

and the resulting simultaneous equations

$$a_o N + a_1 \Sigma x_i = \Sigma Y_i$$

$$a_o \Sigma x_i + a_1 \Sigma x_i^2 = \Sigma x_i Y_i$$

were solved for a_o and a_1.

The equation of the line then became:

$$\text{Ln } \overline{Nu} = a_o + a_1 \text{Ln Re}$$

or

$$\overline{Nu} = e^{a_o} \text{ Re}^{a_1}$$

The standard error for the present study correlation was calculated by the following equation:

$$\sigma^2 = \frac{\Sigma(Y_i - y_i)}{N - n - 1}$$

where: Y_i is the actual value of the average Nusselt number obtained experimentally.

y_i is the value of the average Nusselt number calculated from the correlation equation.

N is the number of data points used in the correlation.

n is the degree of the polynomial used.

For the present study the following correlation was obtained for the straight section:

$$\overline{Nu} = .063\ Re_{hd}^{0.65}$$

with a standard error of:

$$\sigma^2 = 0.1988$$

The correlation obtained for the curved section was:

$$\overline{Nu} = .040\ Re_{hd}^{0.72}$$

and its standard error was determined to be:

$$\sigma^2 = 0.1050$$

LIST OF REFERENCES

1. Taylor, G. I., "Stability of a Viscous Liquid Contained Between Two Rotating Cylinders," Philosophical Transactions of the Royal Society of London, series A, V.233, pp. 289-343, 1923.

2. National Advisory Committee for Aeronautics, Technical Memorandum 1375, On the Three Dimensional Instability of Laminar Boundary Layers on Concave Walls, by H. Gortler, 1942.

3. Smith, A.M.O., "On the Growth of Taylor-Gortler Vortices Along Highly Concave Walls," Quarterly of Applied Mathematics, V. 8, pp. 233-263, November 1955.

4. Dement'eva, K. V. and Aronov, I. Z., Hydrodynamics and Heat Transfer in Curvelinear Channels of Rectangular Cross Section. Journal of Engineering Physics, V. 34, No. 6, pp. 666-671, 1978.

5. Mayle, R. E., Kopper, F. C., Blair, M. F., and Bailey, D. A., "Effect of Streamline Curvature on Film Cooling," Journal of Engineering for Power, Trans. ASME, V. 99, Series A, No. 1, pp. 77-82, January 1977.

6. Nicolas, J. and LeMeur, A., "Curvature Effects on a Turbine Blade Cooling Film," ASME Paper No. 74-GT-156, 1974.

7. Folayan, C. O. and Whitelaw, J. H., "The Effectiveness of Two-Dimensional Film-Cooling Over Curved Surfaces," ASME Paper No. 76-HT-31, 1976.

8. Lord Raleigh, "On the Dynamics of Revolving Fluids," Proceedings of the Royal Society of London, Series A, V. 93, pp. 148-154, 1916. Reprints in Scientific Papers, V. 6, pp. 447-453.

9. Taylor, G. I., "Distribution of Velocity and Temperature Between Concentric Rotating Cylinders," Proceedings of the Royal Society of London, Series A, V. 151, pp. 494-512, 1935.

10. Dean, W. R., "Fluid Motion in a Curved Channel," Proceedings of the Royal Society of London, Series A, V. 121, pp. 402-420, 1928.

11. Reid, W. H., "On the Stability of Viscous Flow in a Curved Channel," Proceedings of the Royal Society of London, Series A, V. 244, pp. 186-198, 1958.

12. Schlichting, H., Boundary Layer Theory, 7th Ed., pp. 529-536, McGraw-Hill, 1979.

13. Kelleher, M. D., Flentie, D. L., and McKee, R. J., "An Experimental Study of the Secondary Flow in a Curved Rectangular Channel," Journal of Fluids Engineering, V. 102, pp. 92-96, March 1980.

14. Winoto, S. H., Durao, D.F.G., and Crane, R. I., "Measurement within Gortler Vortices," Journal of Fluids Engineering, V. 101, pp. 517-520, December 1979.

15. Aihara, Y., "Nonlinear Analysis of Gortler Vortices," The Physics of Fluids, V. 19, pp. 1655-1660, November 1976.

16. Kreith, F., "The Influence of Curvature on Heat Transfer to Incompressible Fluids," Trans. ASME, V. 77, pp. 1247-1256, 1955.

17. Aerospace Research Laboratories Report ARL 65-68, A Simplified Approach to the Influence of Gortler-Type Vortices on the Heat-Transfer from a Wall, by Leif N. Persen, May 1965.

18. Cheng, K. C., and Akiyama, M., "Laminar Forced Convection Heat Transfer in Curved Rectangular Channels," International Journal of Heat and Mass Transfer, V. 13, pp. 471-490, 1970.

19. Shibani, A. A., and Ozisik, M. N., "A Solution to Heat Transfer in Turbulent Flow Between Parallel Plates," International Journal of Heat and Mass Transfer, V. 20, pp. 65-573, 1977.

20. Mori, Y., Uchida, Y., and Ukon, T., "Forced Convective Heat Transfer in a Curved Channel with a Square Cross Section," International Journal of Heat and Mass Transfer, V. 14, pp. 1787-1805, 1971.

21. Kays, W. M. and Leung, E. Y., Heat Transfer in Annular Passages - Hydrodynamically Developed Turbulent Flow with Arbitrarily Prescribed Heat Flux, International Journal of Heat and Mass Transfer, V. 6, pp. 507-557, 1963.

22. Durao, M. do Carmo, Investigation of Heat Transfer in Straight and Curved Rectangular Ducts Using Liquid Crystal Thermography, Eng. Thesis, Naval Postgraduate School, Monterey, California, 1977.

23. Ballard, J. C. III, Investigation of Heat Transfer in Straight and Curved Rectangular Ducts, Master's Thesis, Naval Postgraduate School, Monterey, California, 1980.

24. Holihan, R. G., Jr., Investigation of Heat Transfer in Straight and Curved Rectangular Ducts for Laminar and Transition Flows, Master's Thesis, Naval Postgraduate School, Monterey, California, 1980.

25. Brinich, P. F. and Graham, R. W., Flow and Heat Transfer in a Curved Channel, NASA Technical Note No. TN-D-8464, 1977.

26. Gebhart, B., Heat Transfer, 2nd Ed., p. 260, McGraw-Hill, New York, 1971.

27. Shah, R. K. and London, A. L., Laminar Flow Forced Convection in Ducts, Supplement 1, pp. 305-312, Academic Press, 1978.

28. Department of Mechanical Engineering, Stanford University, Report No. AHT-3, Heat Transfer with Laminar and Turbulent Flow Between Parallel Planes with Constant and Variable Wall Temperature and Heat Flux, by P. A. McCuen, W. M. Kays, and W. C. Reynolds, 12 April 1962.

29. Kline, S. J. and McClintock, F. A., "Describing Uncertainties in Single-Sample Experiments," Mechanical Engineering, V. 75, pp. 3-8, January 1953.

30. The American Society of Mechanical Engineers, Supplement to ASME Power Test Codes, Chapter 4, Flow Measurement, p. 25, 1959.

31. Gerald, C. F., Applied Numerical Analysis, 2nd Ed., pp. 465-74, Addwon-Waley Publishing Company, 1978.

INITIAL DISTRIBUTION LIST

		No. Copies
1.	Defense Technical Information Center Cameron Station Alexandria, Virginia 22314	2
2.	Library, Code 0142 Naval Postgraduate School Monterey, California 93943	2
3.	Department Chairman, Code 69 Department of Mechanical Engineering Naval Postgraduate School Monterey, California 93943	1
4.	Professor M. D. Kelleher, Code 69Kk Department of Mechanical Engineering Naval Postgraduate School Monterey, California 93943	2
5.	Lieutenant S.F. Daughety, USN Nuclear Reactors Representative Office (NRRO) Norfolk Naval Shipyard Portsmouth, Virginia 23705	2

206176

Thesis
D1634 Daughety
c.1 Experimental investigation of turbulent heat transfer in straight and curved rectangular ducts.